J. Micropalaeontology, 44, 601–632, 2025
https://doi.org/10.5194/jm-44-601-2025


Journal of Micropalaeontology
Open Access

# Low-latitude biostratigraphy and diversity of planktonic foraminifera from the middle Eocene to early Oligocene

**Adam Woodhouse**[1,2,3,7], **Bridget S. Wade**[4], **Tom Dunkley Jones**[1], **Carina Hoorn**[5], **and Kirsty M. Edgar**[1,6]

[1]School of Geography, Earth and Environmental Sciences, University of Birmingham, Birmingham, B15 2TT, UK
[2]School of Earth Sciences, University of Bristol, Bristol, BS8 1RJ, UK
[3]School of Earth and Environmental Sciences, Cardiff University, Cardiff, CF10 3AT, UK
[4]Department of Earth Sciences, University College London, Gower Street, London, WC1E 6BT, UK
[5]Department for Ecosystem Dynamics, Institute for Biodiversity and Ecosystem Dynamics (IBED), University of Amsterdam, 1090 GE Amsterdam, the Netherlands
[6]Lapworth Museum of Geology, University of Birmingham, Birmingham, B15 2TT, UK
[7]School of Environment, Earth and Ecosystem Sciences, Open University, Walton Hall, Kents Hill, Milton Keynes, MK7 6AA, UK

**Correspondence:** Adam Woodhouse (woodhousea2@cardiff.ac.uk)

Received: 25 April 2025 – Revised: 9 October 2025 – Accepted: 19 October 2025 – Published: 2 December 2025

**Abstract.** The middle Eocene through early Oligocene was an important interval for Cenozoic climate evolution, having a substantial impact on global palaeoceanography and the biosphere. At the Eocene–Oligocene Transition (EOT), planktonic foraminifera experienced their highest extinction rates since the Cretaceous–Paleogene mass extinction, but the exact extinction mechanisms are poorly constrained. Low-latitude sites that span the EOT are particularly rare in part because of poor preservation of carbonate in many ocean basins in the Eocene. Here we present new planktonic foraminiferal assemblage and biostratigraphic data from the Foz do Amazonas Basin located in the western equatorial Atlantic Ocean, shedding light on the biotic response of tropical planktonic foraminifera to long-term planetary cooling and the establishment of Antarctic glaciation. The samples yielded a rich planktonic foraminiferal assemblage totalling 116 species, enabling the recognition of three Cenozoic tropical planktonic foraminiferal zones (E9, E10, E14) across the middle Eocene–early Oligocene ( $\sim$ 44–34 Ma), with several intervals undifferentiated. Assemblages indicate increased upwelling and eutrophication of surface waters possibly associated with fluctuations within water column structure across the EOT. These alterations are likely associated with regional and global perturbations within oceanic circulation and palaeoceanographic variations attributable to the Antarctic glaciations of the earliest Oligocene. The effects of Cenozoic cooling are seen within the planktonic foraminiferal assemblages, wherein a reduction in symbiotic mixed-layer taxa is accommodated by an increase within sub-thermocline dwellers consistent with substantial restructuring of oceanic stratification through the EOT and cold-water expansion.

## 1 Introduction

### 1.1 Background

The Paleogene Epoch (66.06–23.03 Ma) was a critical interval in Cenozoic climate evolution. It encompassed the global greenhouse climate of the Palaeocene–late Eocene, including the peak interval of sustained Cenozoic warmth, the Early Eocene Climatic Optimum (EECO; 53.3–49.1 Ma; Inglis et al., 2020). The EECO was succeeded by a gradual global cooling trend which continued to the end of the Pleistocene and was punctuated by multiple cooling events, most notably the Eocene–Oligocene Transition (EOT), an $\sim$ 790 kyr cooling interval that straddled the Eocene–Oligocene Boundary (EOB; 33.9 Ma; Pearson and Burgess, 2008; Zachos et

al., 2001; Thomas, 2008; Liu et al., 2009; Pross et al., 2012 ; Hyland and Sheldon, 2013; Passchier et al., 2013; Inglis et al., 2015; Westerhold et al., 2020; Hutchinson et al., 2021). Due to cooling, changes within global water column temperature and structure following the EECO contributed to a spur in evolutionary and morphological innovation amongst the planktonic foraminifera through the creation and invasion of new depth habitats (Norris, 1991; Schmidt et al., 2004a, b). During the middle Eocene, there was a progressive shift in the dominance from cosmopolitan taxa to more specialized symbiotic forms within (sub)tropical latitudes culminating in the highest diversity levels since the Cretaceous–Paleogene mass extinction event (Pearson et al., 2006a; Aze et al., 2011; Ezard et al., 2011; Fraass et al., 2015; Lowery et al., 2020; Swain et al., 2024). The mid-Eocene diversity peak was swiftly followed by the disappearance of many of the major mixed-layer, symbiont-bearing groups through the middle and late Eocene, including the iconic *Morozovelloides*, large acarininids, and *Globigerinatheka*, followed by a further dramatic loss of diversity ($\sim 35\,\%$ species-level extinction) across the EOT, particularly amongst *Hantkenina* and *Turborotalia* (Aze et al., 2011; Ezard et al., 2011; Wade et al., 2018a; Lowery et al., 2020). The most likely extinction mechanism is water column restructuring associated with progressive global cooling (Boersma et al., 1987; Keller et al., 1992; Thomas, 2008, Wade and Pearson, 2008; Ezard et al., 2011; Katz et al., 2011; Houben et al., 2019), though many environmental and ecological stressors were likely at play. Early Oligocene faunas are notably less morphologically and ecologically specialized than those within the Eocene, and the clade took $\sim 10$ million years (Myr) to regain its lost complexity (Wade et al., 2018a), though species diversity did not recover until much later in the Pliocene (Fraass et al., 2015 ; Lowery et al., 2020; Swain et al., 2024; Woodhouse, 2025). The spatial pattern of local extinction and change across the EOT is not as well known, in part because low-latitude records can be comparatively lacking compared to the middle latitudes (Fig. 1; Fenton et al., 2021; Woodhouse, 2021); when present, they are commonly affected by poor recovery (e.g. Winterer et al., 1971; Fleisher, 1974), unconformities (e.g. Beckman, 1972; Fleisher, 1974; Saito, 1985), poor preservation/dissolution (e.g. Fleisher, 1974; Leckie et al., 1993; Pearson et al., 1997), and depauperate/barren assemblages (e.g. Douglas, 1973; McGowran, 1974; Expedition 320/321 Scientists, 2010a, b, c). Furthermore, some regions may simply be understudied (e.g. Krashininnikov, 1971; Douglas, 1973). Rare exceptions do exist within the Indian and western Pacific oceans which showcase good preservation of calcareous microfossils suitable for geochemical analyses that contribute to deciphering the regional patterns of low-latitude ecosystem change (Wade and Pearson, 2008; Pearson and Wade, 2015; Jones et al., 2019; Jones and Dunkley Jones, 2020; Coxall et al., 2021). Thus, this study seeks to explore planktonic foraminiferal macroevolutionary responses across the EOT within the western equatorial Atlantic Ocean and contextualize them on the global scale to better determine how the environmental changes associated with this critical interval of cryosphere evolution affected the water column and its inhabitants.

### 1.2 Regional and stratigraphic setting

The Algodoal Well, or "Well 2" (3°2′58.660″ N–47°44′45.801″ W; Figs. 1 and 2) is located within the southeastern interior of the Foz do Amazonas Basin, a large basin covering $> 360\,000\,\mathrm{km}^2$, spanning the continental shelf, slope, and deep-water regions (Mello et al., 2001; Mohriak, 2003; Pasley et al., 2005; Figueiredo et al., 2009; Hoorn et al., 2017) in the northern area of the Brazilian equatorial margin (Figs. 1 and 2). The basin has undergone only minimal deviations in its palaeolatitudinal position since the Early Cretaceous, remaining close to the Equator (Müller et al., 2016), and the recovered sequence represents a substantial proportion (by thickness) of the Upper Cretaceous–Holocene drift megasequence which formed after the divergence of the African and South American plates beginning in the Aptian ($\sim 125$ Ma; Castro et al., 1978; Mello et al., 2001; Heine et al., 2013; Duarte et al., 2025). The Algodoal Well was drilled by the Brazilian petroleum company, Petróleo Brasileiro S.A. (Petrobras), at 754 m water depth from a drilling table situated 25.5 m above sea level (a.s.l.) and recovered $> 5000$ m of sediments spanning the Pleistocene to middle Eocene. These drilling depths are unachievable via conventional scientific ocean drilling, showcasing the utility of industry collaboration for investigating deeply buried sediments (Fig. 2). Sediments can be lithostratigraphically subdivided into the Marajó, Amapá, and Travosas formations, which are characterized by nonmarine and proximal shallow-marine clastics, shallow (shelf) marine carbonates, and distal fine-grained sediments, respectively (Brandão and Feijó, 1994; Mello et al., 2001; Pasley et al., 2005; Figueiredo et al., 2009). The sediments within this study are sourced from the Travosas Formation, interpreted to occupy a bathyal water depth (Brandão and Feijó, 1994).

Ditch cutting samples were provided by Petrobras and sourced from 5269–5509 m below the drilling table (bdt), spanning the middle Eocene through early Oligocene within the Travosas Formation. Ditch cutting samples are inherently affected by the methodology of their collection, where the drilling fluid flowing up the borehole containing actively sampled cuttings may mix with cuttings from multiple higher stratigraphic horizons within the borehole (Bown et al., 2022). Potential mixing should always be considered when interpreting stratigraphic data from ditch cuttings; however, previous work at this site showcases the utility of these sediments for palaeoclimatic, palaeoceanographic, and micropalaeontological studies (Figueiredo et al., 2009; Hoorn et al., 2017; Lammertsma et al., 2018).

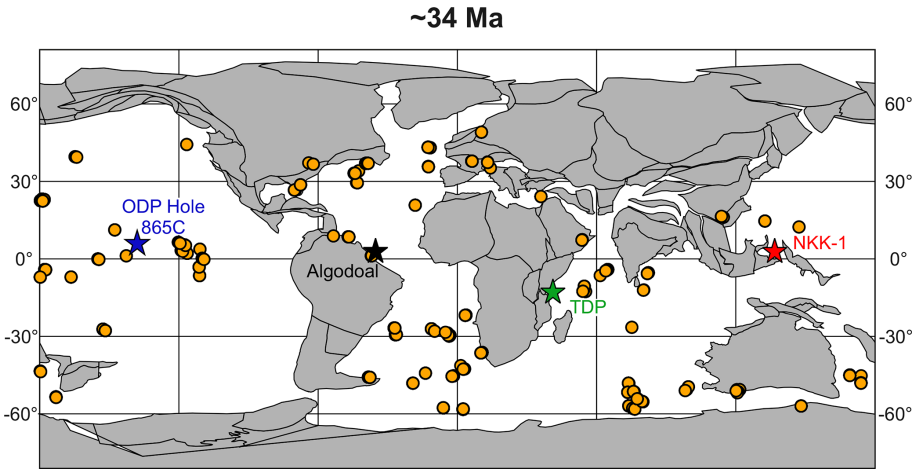


**Figure 1.** Global palaeogeographic reconstruction at ~ 34 Ma, the Eocene–Oligocene Transition, displaying the global distribution of sites covering the interval from 35–33 Ma from the Triton dataset (Fenton et al., 2021). The positions of the Algodoal Well and ODP Hole 865C used in this study are marked, as are important low-latitude localities including the Tanzania Drilling Project (TDP; Pearson and Wade, 2015) and Nanggulan NKK-1 (Coxall et al., 2021) sites.

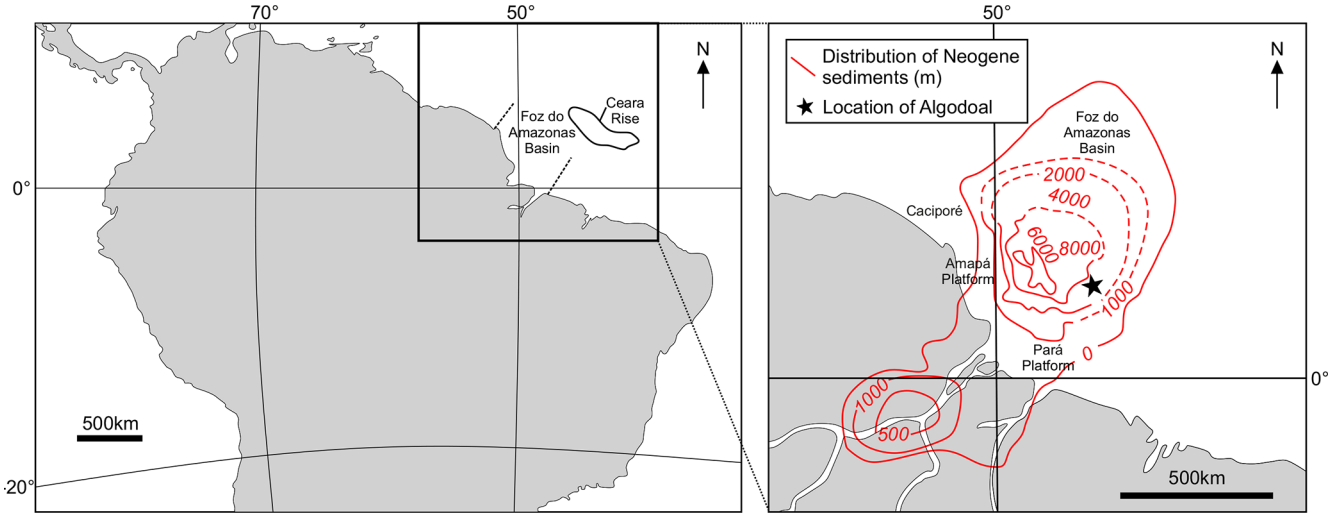


**Figure 2.** Regional context of the Foz do Amazonas Basin and the Algodoal Well showing the total thickness of overlying Neogene sediments, indicating their regional distribution (modified from Mello et al., 2001; Hoorn and Wesselingh, 2010).

We generated planktonic foraminiferal assemblage data from the Algodoal Well to (1) construct a planktonic foraminiferal biostratigraphic scheme within the Foz do Amazonas Basin, (2) assess the preservation of planktonic foraminiferal shells and thus suitability for geochemical investigations, and (3) investigate changes in generic and functional group diversity of planktonic foraminifera during the "greenhouse–icehouse" world transition.

## 2 Materials and methods

### 2.1 Sample processing

A total of 20 ditch cutting samples spanning 5269–5509 mbdt consisting primarily of coarse–fine-grained greyish-green siliciclastic material were provided by Petrobras along with a nannoplankton biostratigraphic scheme created on site by Varol (2004) during the drilling of the Algodoal Well (Table S1 in the Supplement), which were recalibrated to the scheme of Agnini et al. (2014) supplemented by Fornaciari et al. (2010). Samples were processed at the University of Bristol School of Earth Sciences by drying them in a low-temperature (< 50 °C) oven for approximately 1 week

until the dry bulk sediment weight stabilized. Subsequently, they were soaked in Milli-Q water for 30 min prior to washing over a 63 µm sieve and then placed in a low-temperature drying oven overnight. However, samples were clay-rich and relatively consolidated, so 16 of the samples required further treatment and were subsequently placed within a glass flask, submerged in Calgon, and placed on a shaker table operating at ∼ 60 rpm for 48 h to aid disaggregation. Samples were then removed from the Calgon solution and washed over a 63 µm sieve with deionized water before being dried. Following this, the > 63 µm fraction was weighed and the weight % coarse fraction was calculated (see Hancock and Dickens, 2005).

### 2.2 Assemblage analysis

Once dry, 10 of the samples were selected (every other sample) for detailed planktonic foraminiferal assemblage analysis in the micropalaeontological laboratories at the School of Geography, Earth and Environmental Sciences at the University of Birmingham. Samples were dry-sieved to remove the > 500 µm (which still contained consolidated lumps of bulk sediment) and 63–125 µm fractions following the findings of Al-Sabouni et al. (2007) that tropical assemblage diversity is well represented by the 125–500 µm sieve size fraction. The 125–500 µm fraction used for assemblage analysis was split with a micro-splitter until a subsample containing ∼ 300 individual planktonic foraminifera was achieved. Following the full picking and assemblage count of the split fraction, the remainder of both the 125–500 µm sample and the > 500 and < 125 µm sieve size fractions were scanned for rare and biostratigraphically important taxa. This scanning was repeated for the 10 samples that were not selected for full assemblage counts to create a continuous biostratigraphic record. Planktonic foraminifera were identified to species level unless specified using the taxonomy of Pearson et al. (2006b), Spezzaferri (1994), Pearson and Wade (2015), Huber et al. (2016), and Wade et al. (2018b). Taxa were later grouped by genus to assess evolutionary trends through the study section.

A semi-quantitative preservation index was used to determine variations in planktonic foraminiferal shell preservation as follows: 5 = very good (specimens mostly whole, very well preserved ornamentation and surface ultrastructure, no visible modification of the shell wall); 4 = good (specimens often whole, ornamentation and surface ultrastructure preserved but sometimes abraded or overgrown, visible evidence of modification of the shell wall); 3 = moderate (specimens often etched or broken, ornamentation and surface ultrastructure modified, majority of specimens identifiable to species level); 2 = poor (most specimens crushed or broken, recrystallized, diagenetically overgrown, or infilled with crystalline calcite; most specimens difficult to identify to species level); and 1 = very poor (all specimens crushed or broken, recrystallized, diagenetically overgrown, or infilled with secondary minerals; most specimens difficult to identify to genus level).

The percentage of planktonic foraminifera relative to total foraminifera was determined in the 10 assemblage count samples from the 125–500 µm sieve size fractions to determine relative oceanicity (higher planktonic foraminifera % corresponding to higher oceanicity/water depth; van der Zwaan et al., 1990; Hayward et al., 1999). Absolute abundance (number of specimens per gram bulk sediment, *n*/g) of the planktonic foraminiferal component was also recorded by counting all specimens in the analysed sediment fraction.

To determine changes in the ecological structure of planktonic foraminiferal communities through time, all foraminifera were assigned to ecological groups (ecogroups) based on Aze et al. (2011; see Table S2) for macroperforate planktonic foraminiferal species. This scheme separates planktonic foraminifera life strategies into six distinct ecogroups on the basis of species-specific biogeographic distributions and the stable oxygen ($\delta^{18}O$) and carbon ($\delta^{13}C$) isotopic signatures of their shells (Table 1). The ecogroup assignments of Aze et al. (2011) were updated from the literature where necessary due to recent taxonomic revisions (Poore and Matthews, 1984; Barrera and Huber, 1991; Pearson et al., 1993; 2001, 2018a; Van Eijden and Ganssen, 1995; Olsson et al., 2006; Pearson and Wade, 2009; Moore et al., 2014; Coxall and Spezzaferri, 2018; Spezzaferri et al., 2018; Wade et al., 2018c, d). Microperforate and medioperforate taxa which were not included in Aze et al. (2011) were also assigned to respective ecogroups (Boersma and Shackleton, 1977; Liu et al., 1997; Pearson et al., 2001, 2018; Majewski, 2003; Huber et al., 2006; Pearson and Wade, 2009; Luciani et al., 2010). No high-latitude forms (Ecogroup 5) were found within our study. The relative abundances of planktonic foraminiferal ecogroups can provide detail on water column structure in ancient environments across a variety of spatiotemporal scales (Boscolo-Galazzo et al., 2021, 2022; Woodhouse et al., 2021, 2023a, b; Swain et al., 2024).

### 2.3 Statistical analysis

Species richness and Shannon's index ($H'$) (Shannon and Weaver, 1949) were employed to assess species assemblage dynamics through time and, more specifically, assemblage diversity and distribution across the study interval. Species richness shows the raw number of species per sample: Shannon's index ($H'$) takes into account both the richness and the number of individuals of each species; it varies from 0 for communities with a single species to higher values for communities with many species and a more even distribution of individuals between present species. We used multidimensional scaling and correspondence analysis (CA) (Parker and Arnold, 2003) to identify any distinct temporal groupings of planktonic foraminifera assemblages during the study interval.

**Table 1.** Ecogroup codes assigned to planktonic foraminifera based on Aze et al. (2011). See the full list used in this study in Table S2.

| Ecogroup code | Description |
|---|---|
| 1 | Open-ocean mixed layer tropical/subtropical, with symbionts |
| 2 | Open-ocean mixed layer tropical/subtropical, without symbionts |
| 3 | Open-ocean thermocline |
| 4 | Open-ocean sub-thermocline |
| 5 | High latitude |
| 6 | Upwelling/high productivity |

### 2.4 Imaging

Several representative specimens of key biostratigraphic markers and common taxa were selected from within the sampling interval for reflected light microscopy (RLM) and scanning electron microscopy (SEM), alongside specimens from Ocean Drilling Program (ODP) Hole 865C, for comparative textural and preservational analysis of Algodoal specimens with "frosty" (recrystallized) specimens (e.g. Sexton et al., 2006a; Edgar et al., 2015). For RLM, specimens were mounted on SEM stubs and imaged both dry and submerged in water using a Zeiss AxioCam ICc 1 attached to a Zeiss SV 11 microscope at the School of Geography, Earth and Environmental Sciences, University of Birmingham. Additional RLM imaging was taken in the Department of Earth Sciences, University College London. Selected specimens were imaged with the use of an Olympus SZX16 stereo microscope, equipped with a DP73 multifocal camera. The software Stream Motion (Olympus) was used to stack the images.

Prior to SEM imaging, specimens were ultrasonicated in deionized water for 3–10 s to remove particulates, dried, and then mounted upon an SEM stub. Specimens were analysed through secondary electron imaging, where those imaged on Plate 3 were sputter-coated in gold–palladium, whilst all others were uncoated. To investigate internal features and shell walls in cross-section, whole specimens were placed upon a wetted glass slide and broken using pressure from another (see method in Pearson et al., 2015). The fragments were then mounted alongside whole specimens on the SEM stub. Scanning electron microscopy of Plate 3 specimens was conducted at Cardiff University School of Earth and Environmental Sciences with a Veeco FEI (Phillips) XL30 ESEM, and all other specimens were analysed at the University of Birmingham School of Geography, Earth and Environmental Sciences on a Phenom ProX desktop SEM.

### 2.5 Comparison to global datasets

To investigate how planktonic foraminiferal macroevolution and palaeoecology developed globally over the study interval in comparison to the Algodoal Well, the Triton dataset (Fenton et al., 2021) was downloaded, and all planktonic foraminiferal records from 45–25 Ma (including our study interval) were binned into 20 time bins with equal length (1 Myr). Species were assigned the speciation and extinction datums in accordance with Aze et al. (2011) and Fenton and Woodhouse et al. (2021), and all species occurrences located outside of these assigned stratigraphic ranges were removed. This range trimming eliminated occurrence data likely attributable to misidentification and/or reworking that may create artificial "tails" within speciation and extinction data (Liow et al., 2010; Lazarus et al., 2012; Flannery-Sutherland et al., 2022). The trimming of taxa resulted in a final dataset with 36 396 planktonic foraminiferal occurrences. All species were assigned to their respective ecogroups using the methods described in Sect. 2.2. (see Table 1).

## 3 Results

### 3.1 Foraminiferal preservation

Sample-specific observations revealed generally good to moderate foraminiferal shell preservation throughout the section but with preservation improving up-section (Fig. 3, Plates 1–5). Preliminary observations of the planktonic foraminifera within the early Oligocene–latest Eocene (5269–5311 mbdt) of Algodoal indicated a number of specimens exhibiting "glassy" preservation (Plate 4; Pearson et al., 2001; Sexton et al., 2006a; Bown et al., 2008; Edgar et al., 2015). SEM analysis however, showed variable degrees of diagenesis and corrosion/abrasion, and almost all specimens appear to have obscured apertures due to infilling (e.g. Plate 2, specimen 4). Wall texture is a key diagnostic feature for planktonic foraminifera taxonomy, and SEM comparisons with muricae-bearing genera from ODP Hole 865C indicate that Algodoal specimens of *Acarinina* and *Morozovelloides* consistently exhibit blunted or broken muricae (Plate 3). Whether this is mechanical damage or a product of dissolution is unknown. No individuals within Algodoal exhibited "frosty" preservation comparable to those from ODP Hole 865C (Plate 4). Investigation of cross-sections of specimen shell walls from 5269 mbdt (early Oligocene) indicate preservation of the original shell architecture evidenced by cohesive sub-micron-scale crystallites (microgranules sensu Blow, 1979) with biogenic layers lacking

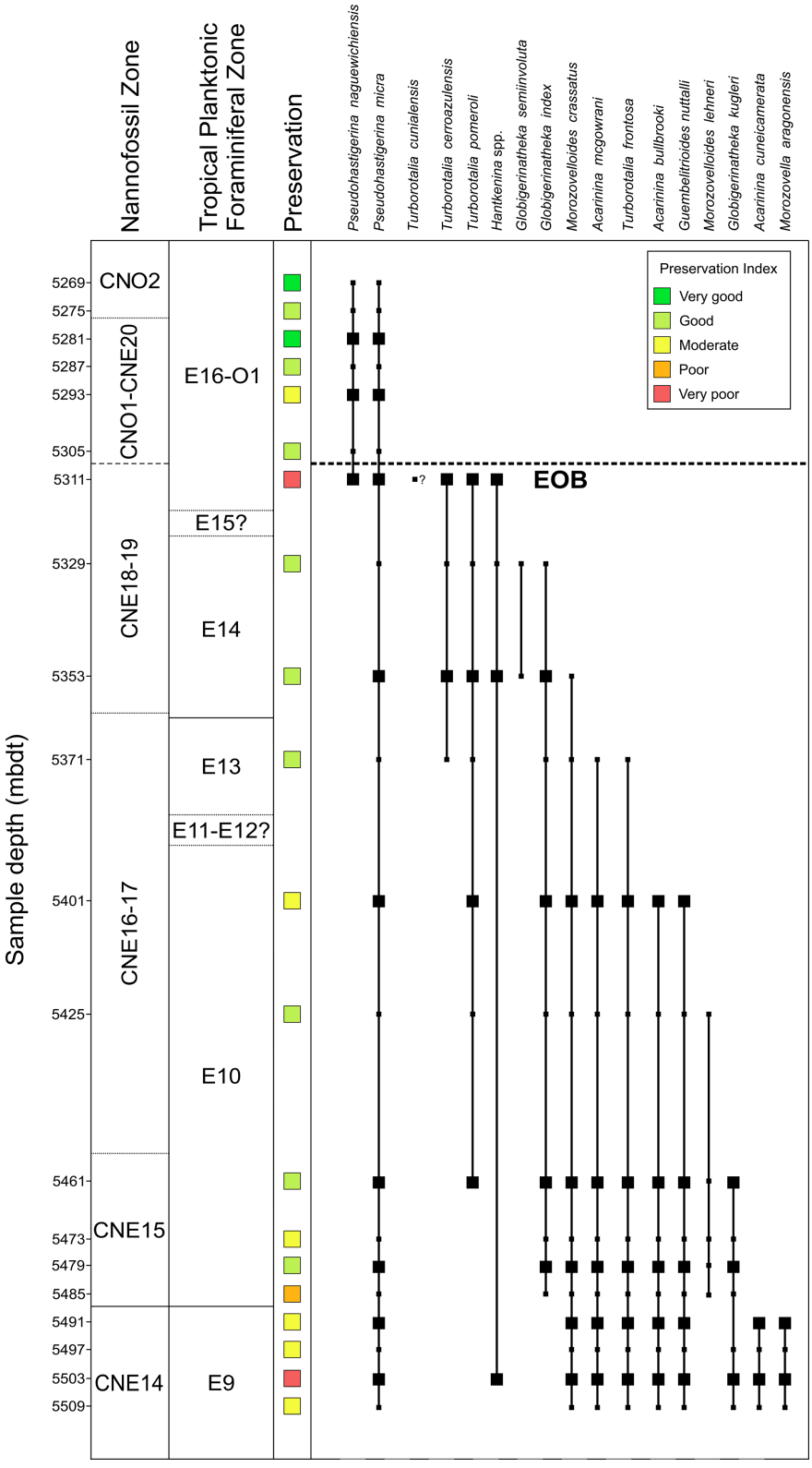


**Figure 3.** Middle Eocene–early Oligocene record of biostratigraphically important planktonic foraminiferal taxa, preservation within the Algodoal Well, and the interpreted position of the EOB. Large squares = taxa recorded within assemblage counts; small squares = taxa recorded outside population counts; solid lines = confident boundaries; dashed lines = probable boundaries, stippled lines = possible boundaries. Nannofossil zonation is based on Varol (2004); see Hoorn et al. (2017) or Lammertsma et al. (2018). Planktonic foraminiferal zonation is based on Wade et al. (2011). See Table S3 for biostratigraphic events.

gaps (Plate 4). In contrast, specimens from ODP Hole 865C (Plate 4) show loosely packed crystals on the shell surface and interior, along with minor overgrowth of external muricae by blade-like crystals (see Edgar et al., 2015). Despite the well-preserved internal wall structures at Algodoal, the presence of large-scale overgrowth and/or infilling of entire chambers and pore canals by inorganic calcite (Plate 4) hinders Algodoal's potential as a site of exceptional preservation and for reliable geochemically derived sea surface temperatures and other geochemical proxies. Notably, similar preservation has been documented at NKK-1 in central Java where reliable geochemical data were intermittently extracted in better-preserved intervals (Coxall et al., 2021).

Within the supplementary data provided by Petrobras, two organic-rich intervals were documented from 5251–5311 mbdt (EOT and early Oligocene) and from 5455–5509 mbdt (middle Eocene) (herein referred to as ORG-1 and ORG-2, respectively; Figs. 4–7). These intervals contain relatively abundant pyritized detrital grains, along with foraminiferal shells displaying variable levels of pyritization varying from minor to whole replacement, noticeably more prominent in ORG-1. Furthermore, within ORG-1, infrequent shells were observed exhibiting significant morphological abnormalities such as significant chamber enlargement/deformation (Plate 3).

### 3.2 Planktonic foraminiferal biostratigraphy

We identified 116 species of planktonic foraminifera belonging to 30 genera (Fig. 3; Table S4), permitting the identification or estimation of three Cenozoic tropical planktonic foraminiferal zones (Wade et al., 2011) in the early Oligocene to middle Eocene (zones E14, E10, and E9) (Fig. 3; Table 2). Accurate assignment of zones O1, E16, E15, E13, E12, and E11, however, was not possible due to rare/missing marker species (e.g. *Hantkenina*, *Orbulinoides beckmanni*) and/or low sampling resolution, so they were left undifferentiated. Absolute ages are as per the Geological Time Scale 2012 (Anthonissen and Ogg, 2012; Gradstein et al., 2012; Vandenberghe et al., 2012).

*Pseudohastigerina naguewichiensis* Highest-occurrence Zone (Zone O1) to *Hantkenina alabamensis* Highest-occurrence Zone (Zone E16) (Undifferentiated), 32.1–34.61 Ma, 5269–5311 mbdt

Zone O1 is defined between the highest occurrence (Top) of the nominate taxa *P. naguewichiensis* (32.1 Ma) and Top of *Hantkenina alabamensis* (33.89 Ma). The top of Zone O1 was not identified because *P. naguewichiensis* was present in the topmost studied sample at 5269 mbdt. The base of Zone O1 could not be confidently determined because of the rarity of *Hantkenina* at the site. However, the Eocene–Oligocene Boundary (EOB; ∼ 33.9 Ma) likely falls between 5305–5311 mbdt. Zone E16 is defined by the partial range of the nominate taxon between the Tops of *H. alabamensis* (33.89 Ma) and *G. index* (34.61 Ma) (Fig. 3). Rare hantkeninids throughout the section required the use of secondary markers to estimate the top of Zone E16 and the EOB, where an abrupt reduction in the size and abundance of *P. micra* (∼ 33.89 Ma; Wade and Pearson, 2008; Miller et al., 2008; Wade and Olsson, 2009; Pearson and Wade, 2015; Coxall et al., 2021) suggests that the zone boundary lies between 5305–5311 mbdt. The presence of *Turborotalia cerroazulensis* and a possible specimen of *Turborotalia cunialensis* at 5311 mbdt supports this assignment, as both forms become extinct just below the boundary (Pearson et al., 2006c). However, the base of *T. cunialensis* has been noted to be problematic due to taxonomic inconsistencies (Wade and Cheng, 2024). The calibration of the Top of *T. cerroazulensis* to 34.03 Ma and lack of *G. index* also constrains the sample at 5311 mbdt to within Zone E16 (34.03–34.61 Ma; Berggren and Pearson, 2005; Wade et al., 2011). The co-occurrence of *G. index* and *G. semiinvoluta* within the underlying sample from 5329 mbdt indicating Zone E14 prevented the identification of Zone E15, which may be present between 5311–5329 mbdt assuming continuous sedimentation throughout the interval.

*Globigerinatheka semiinvoluta* Highest-occurrence Zone (Zone E14), 36.18–38.25 Ma, 5329–5353 mbdt

Zone E14 is the interval between the Top of the nominate taxa *Globigerinatheka semiinvoluta* (36.18 Ma) and the Top of *Morozovelloides crassatus* (38.25 Ma). Within the Algodoal section, Zone E14 is represented by an ∼ 24 m interval (5329–5353 mbdt). The total stratigraphic range of *G. semiinvoluta* is confined within the boundaries of this zone, wherein the nominate taxon originates (37.54 Ma) after the Top of *M. crassatus* (38.25 Ma; Wade et al., 2011, 2012, 2021). A single specimen of *M. crassatus* was found at 5353 mbdt, possibly marking it as close to the base of Zone E14. The apparent lack of *A. mcgowrani* within this sample may be attributable to the rapid decline and rarity of the larger acarininids towards the top of Zone E13 (Wade, 2004).

*Morozovelloides crassatus* Highest-occurrence Zone (Zone 13) to *Morozovelloides lehneri* Partial-range Zone (Zone E11) (Undifferentiated), 38.25–42.07 Ma, 5353–5371 mbdt

Zone E13 is defined as the interval between the Top of the nominate taxa *Morozovelloides crassatus* (38.25 Ma) and the Top of *Orbulinoides beckmanni* (40.03 Ma). The sample at 5353 mbdt may represent upper Zone E13 due to the Top of *M. crassatus* in this sample (38.25 Ma; see Zone E14 description), where the absence of the secondary marker *Acarinina mcgowrani* (Top at 38.62 Ma) may suggest an age range of 38.25–38.62 Ma. The sample from 5371 mbdt yielded secondary markers *Acarinina mcgowrani* (Top at 38.62 Ma) and *Turborotalia frontosa* (Top at 39.42 Ma) that go extinct within Zone E13 (Wade et al., 2011), which, together with an

**Table 2.** Planktonic foraminiferal biostratigraphic datums used in this study are from the Geological Time Scale 2012 (Anthonissen and Ogg, 2012; Gradstein et al., 2012; Vandenberghe et al., 2012). Calcareous nannofossil biostratigraphic datums are from Agnini et al. (2014) and Fornaciari et al. (2010). Depth value in parentheses indicates the mid-point depth. Top = highest occurrence; Top Common = highest common occurrence; Base = lowest occurrence; PF = planktonic foraminifera; CN = calcareous nannofossil.

| Datum | Type | Age (Ma) | Depth (mbdt) | Reference |
|---|---|---|---|---|
| Top *Reticulofenestra umbilicus* | CN (primary) | 32.02 | 5281–5287 (5284) | Agnini et al. (2014) |
| Top Common *Pseudohastigerina naguewichiensis* | PF (secondary) | 33.89 | 5305–5311 (5308) | Wade and Pearson (2008), Miller et al. (2008), Wade et al. (2011) |
| Top *Turborotalia cerroazulensis* | PF (secondary) | 34.03 | 5305–5311 (5308) | Coccioni et al. (1988), Nocchi et al. (1986) |
| Top *Discoaster saipanensis* | CN (primary) | 34.44 | 5305–5311 (5308) | Agnini et al. (2014) |
| Top *Globigerinatheka index* | PF (primary) | 34.61 | 5311–5329 (5320) | Nocchi et al. (1986), Premoli Silva et al. (1988), Berggren (1992) |
| Top *Globigerinatheka semiinvoluta* | PF (primary) | 36.18 | 5311–5329 (5320) | Coccioni et al. (1988), Berggren and Pearson (2005) |
| Top *Chiasmolithus grandis* | CN (secondary) | 37.77 | 5311–5329 (5320) | Agnini et al. (2014) |
| Top *Morozovelloides crassatus* | PF (primary) | 38.25 | 5329–5353 (5341) | Wade et al. (2011) |
| Top *Sphenolithus obtusus* | CN (primary) | 38.47 | 5425–5455 (5440) | Agnini et al. (2014) |
| Top *Acarinina mcgowrani* | PF (secondary) | 38.62 | 5353–5371 (5362) | Wade (2004) |
| Base *Globigerinatheka semiinvoluta* | PF (primary) | 38.62 | 5353–5371 (5362) | Nocchi et al. (1986) |
| Top *Turborotalia frontosa* | PF (secondary) | 39.42 | 5353–5371 (5362) | Berggren et al. (1985) |
| Top Common *Sphenolithus spiniger* | CN (secondary) | 40.27 | 5485–5491 (5488) | Fornaciari et al. (2010), Agnini et al. (2014) |
| Top *Acarinina bullbrooki* | PF (secondary) | 40.49 | 5371–5401 (5386) | Berggren et al. (1985) |
| Top *Guembelitrioides nuttalli* | PF (primary) | ∼ 42.07 | 5371–5401 (5386) | Berggren and Pearson (2005) |
| Base *Turborotalia pomeroli* | PF (secondary) | 42.21 | 5461–5473 (5467) | Berggren et al. (1985) |
| Base *Globigerinatheka index* | PF (secondary) | 42.64 | 5485–5491 (5488) | Stott and Kennett (1990) |
| Base *Morozovelloides lehneri* | PF (secondary) | 43.15 | 5485–5491 (5488) | Berggren et al. (1985) |
| Top *Morozovella aragonensis* | PF (primary) | 43.26 | 5485–5491 (5488) | Berggren et al. (1985) |
| Base *Globigerinatheka kugleri* | PF (primary) | ∼ 43.88 | 5509 | Pearson et al. (2004), Wade et al. (2011) |

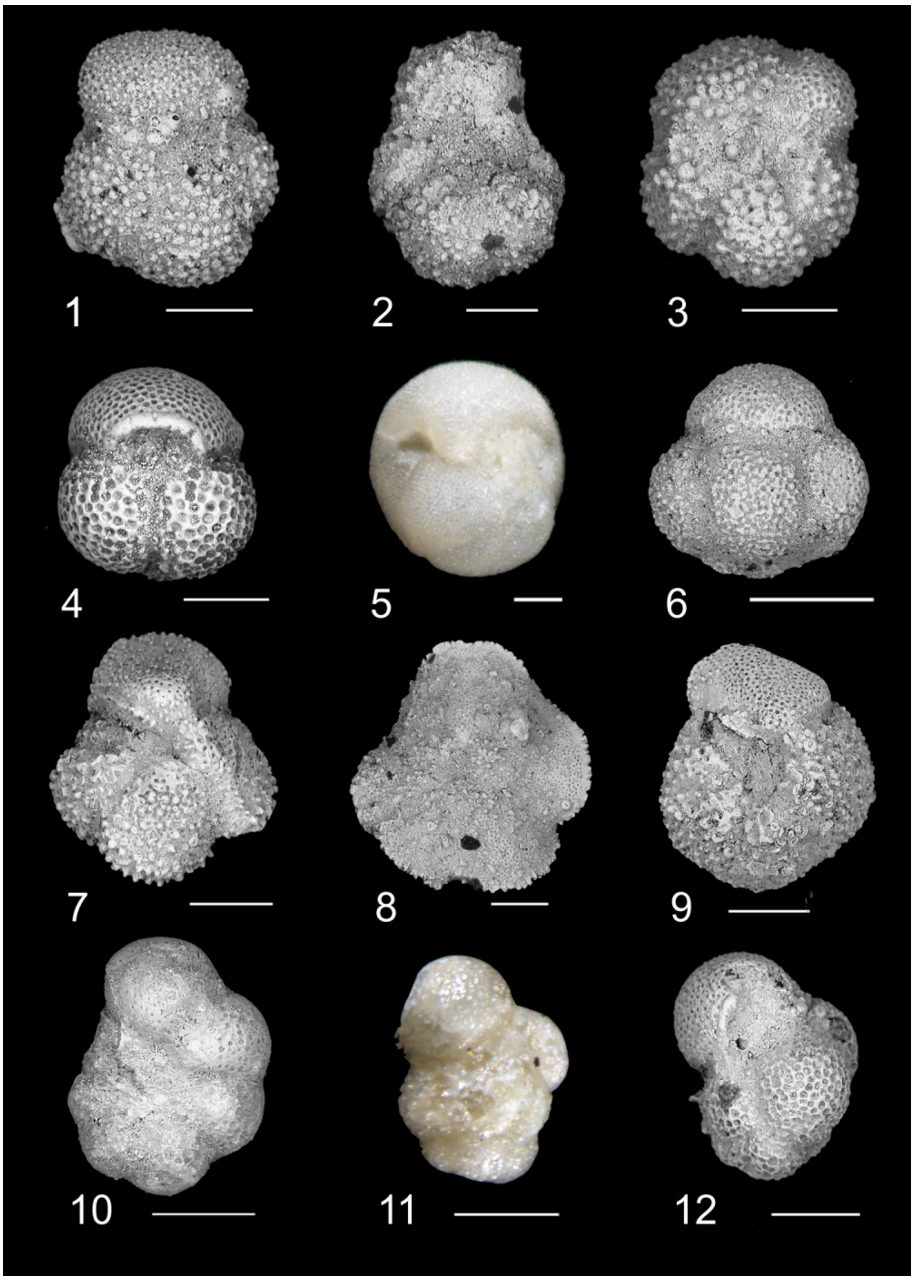


**Plate 1.** Biostratigraphically significant planktonic foraminifera of the Algodoal Well. 1. *Acarinina bullbrooki*. Zone E10, 5401 mbdt. 2. *Acarinina cuneicamerata*. Zone E9, 5491 mbdt. 3. *Acarinina mcgowrani*. Zone E9, 5491 mbdt. 4. *Globigerinatheka index*. Zone E13, 5353 mbdt. 5. *Globigerinatheka semiinvoluta*. Zone E14, 5329 mbdt. 6. *Globigerinatheka kugleri*. Zone E10, 5461 mbdt. 7. *Morozovelloides crassatus*. Zone E9, 5497 mbdt. 8. *Morozovelloides lehneri*. Zone E10, 5485 mbdt. 9. *Morozovella aragonensis*. Zone E9, 5491 mbdt. 10. *Pseudohastigerina micra*. Zones E16–O1, 5311 mbdt. 11. *Guembelitrioides nuttalli*. Zone E10, 5401 mbdt. 12. *Guembelitrioides nuttalli*. Zone E10, 5401 mbdt. All scale bars are 100 µm.

absence of *A. bullbrooki* (its Top at 40.49 Ma is a secondary marker for the base of Zone E12), suggests this sample is located in lower Zone E13 or upper Zone E12. No specimens of *Orbulinoides beckmanni*, the nominate taxon for the underlying *O. beckmanni* taxon range zone (TRZ) E12 (40.03–40.49 Ma), were recorded, preventing confident assignment of both Zone E12 and Zone E11 (Fig. 3). The Middle Eocene Climatic Optimum (MECO; ∼ 40.425 to ∼ 40.023; Krause et al., 2023) is known to occur within this interval and is here approximated to have occurred ∼ 5385 mbdt (Figs. 4–6).

*Acarinina topilensis* Partial-range Zone (Zone E10), 42.07–43.26 Ma, 5401–5485 mbdt

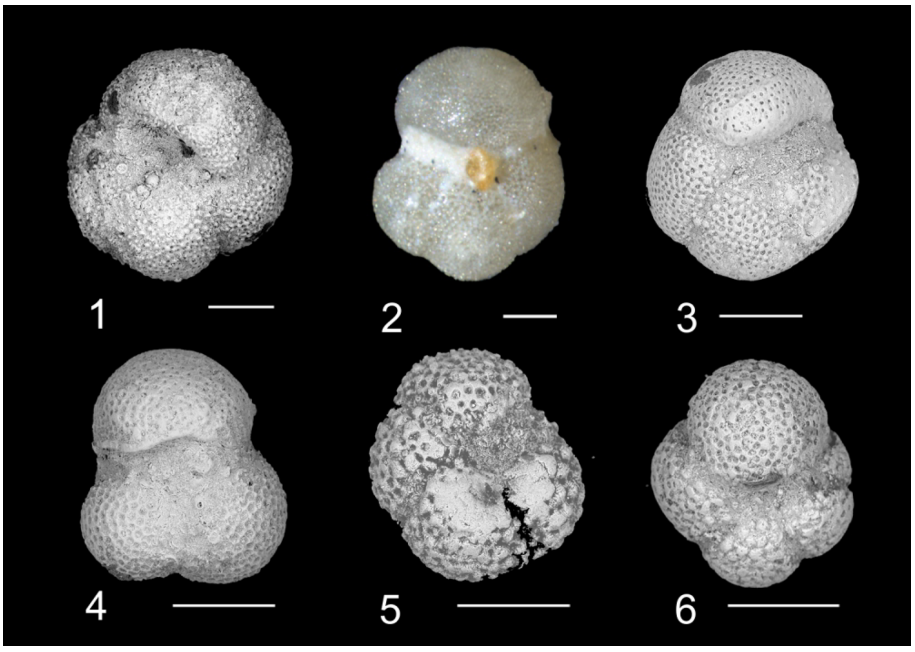


**Plate 2.** Biostratigraphically and taxonomically significant planktonic foraminifera of the Algodoal Well. 1. *Turborotalia pomeroli*. Zone E10, 5461 mbdt. 2. *Turborotalia pomeroli*. Zone E9, 5497 mbdt. 3. *Turborotalia cerroazulensis*. Zone E13, 5353 mbdt. 4. *Turborotalia frontosa*. Zone E9, 5491 mbdt. 5. *Acarinina collactea*. Zones E16–O1, 5311 mbdt. 6. *Paragloborotalia* sp. 1. Zones E16–O1, 5269 mbdt. All scale bars are 100 µm.

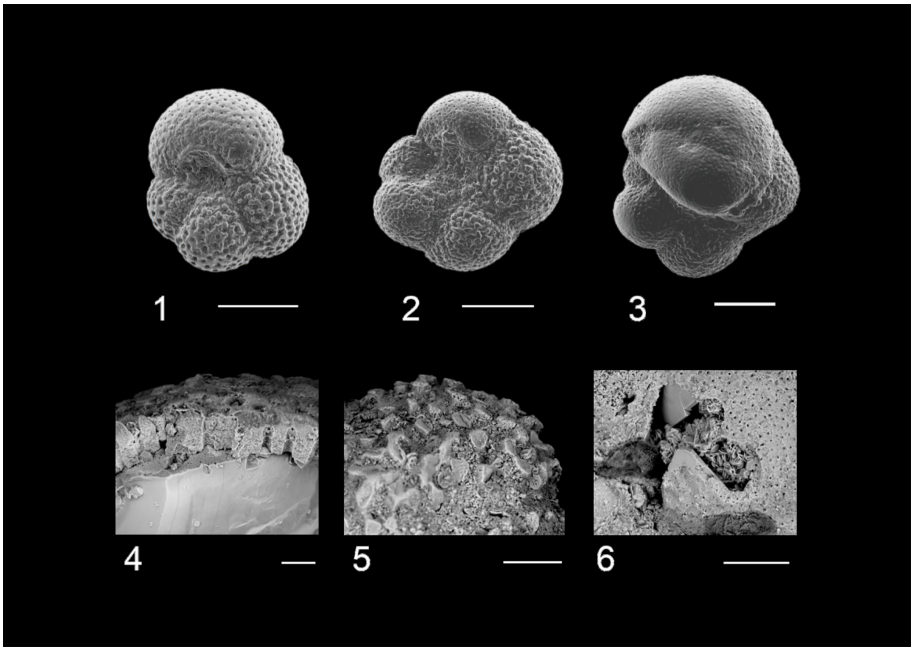


**Plate 3.** Taphonomic and ecological observations within the Algodoal Well. 1. *Turborotalia ampliapertura*, Zone O1, 5269 mbdt. 2–3. *Paragloborotalia nana*, Zone O1, 5269 mbdt (note the abnormal enlargement of the ultimate chamber in 3). 4. Internal wall structure of *Turborotalia* sp, Zones E16–O1, 5269 mbdt (note the preservation of original shell architecture within the cross-section whilst the interior is subjected to significant calcitic infilling). 5. Surface detail of *Morozovelloides crassatus* displaying blunting of muricae common within Algodoal, Zone E9, 5497 mbdt. 6. Surface detail of benthic foraminifera exhibiting infilling with argillaceous material, Zone E9, 5491 mbdt. Scale bars: 1–3, 100 µ; 4, 10 µm; 5–6, 30 µm.

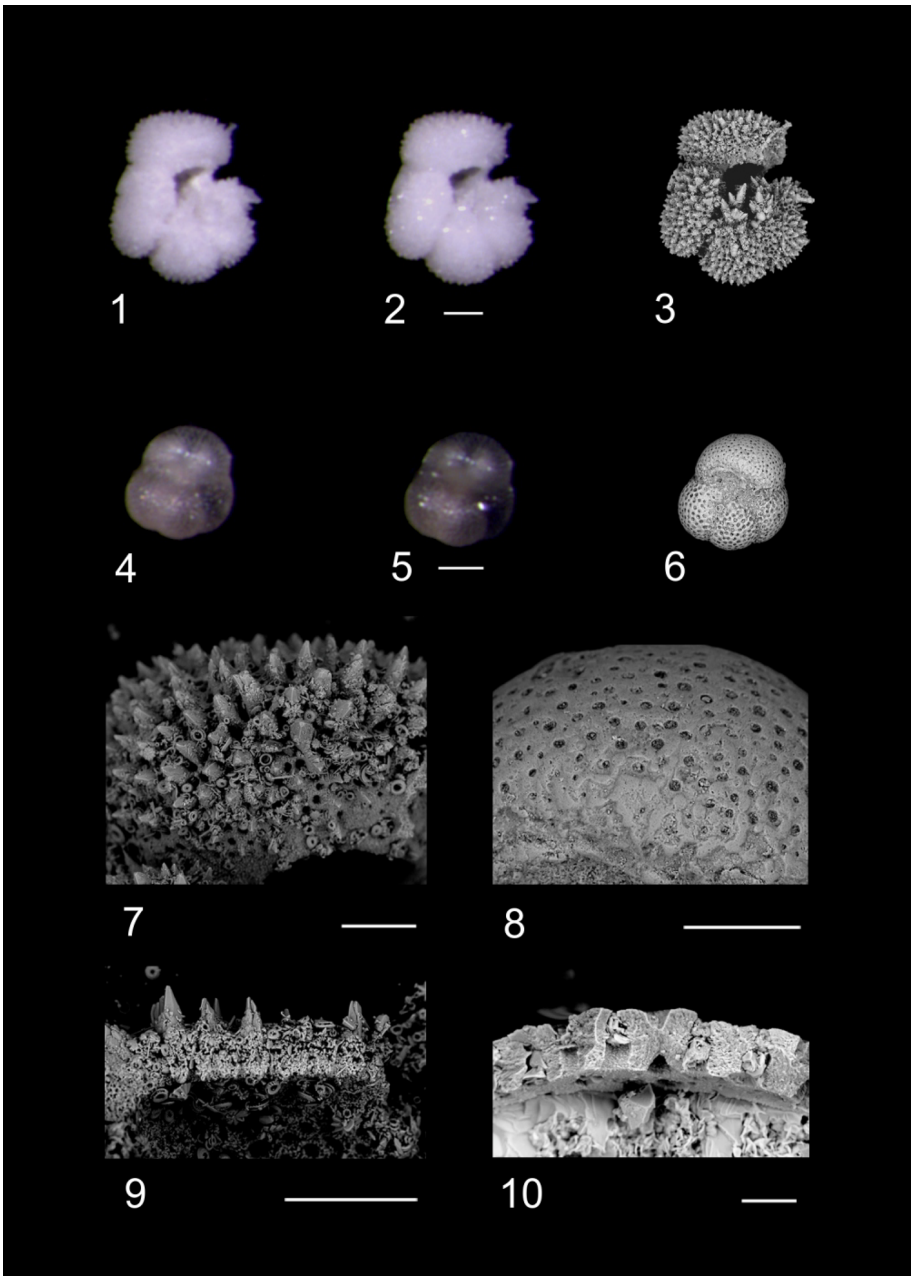


**Plate 4.** RLM and SEM images of planktonic foraminifera contrasting differential preservation characters. RLM photos of specimens dry (1 and 4) and submerged in water (2 and 5) are compared to SEM images of the same specimens (3, 6, 7, 8). 1–3, 7, 9: *Acarinina praetopilensis*, ODP Hole 865C. 4–6, 8, 10: *Turborotalia ampliapertura*. Algodoal, Zones E16–O1, 5269 mbdt. Observational comparisons with RLM displayed some degree of "glassy" preservation within Algodoal (transparency when submerged in DI, e.g. 5). Opacity and apertural infilling were confirmed through SEM as evidence of calcitic infilling (10). Scale bars: 1–6, 100 µm; 7–9, 50 µm; 10, 10 µm.

This is defined by the partial range of the nominate taxa from the Top of *Morozovella aragonensis* (43.26 Ma) to the Top of *Guembelitrioides nuttalli* (∼ 42.07 Ma). The top of Zone E10 was determined between 5371 and 5401 mbdt within the Algodoal section due to the overlapping presence of *G. nuttalli* and *A. bullbrooki* at 5401 mbdt. This does mean that, if Zone E11 is present at the site, it falls between 5371 and 5401 mbdt, where we do not have samples. A total of ∼ 84 m is assigned to Zone E10, with the base situated between 5485–5491 mbdt represented by the Top of *M. aragonensis* (43.26 Ma) at 5491 mbdt. A Zone E10 assignment also fits with the assemblages reported in the samples in between the main datums with overlapping occurrences of *T. pomeroli* (base at 42.21 Ma in Zone E10) and the con-

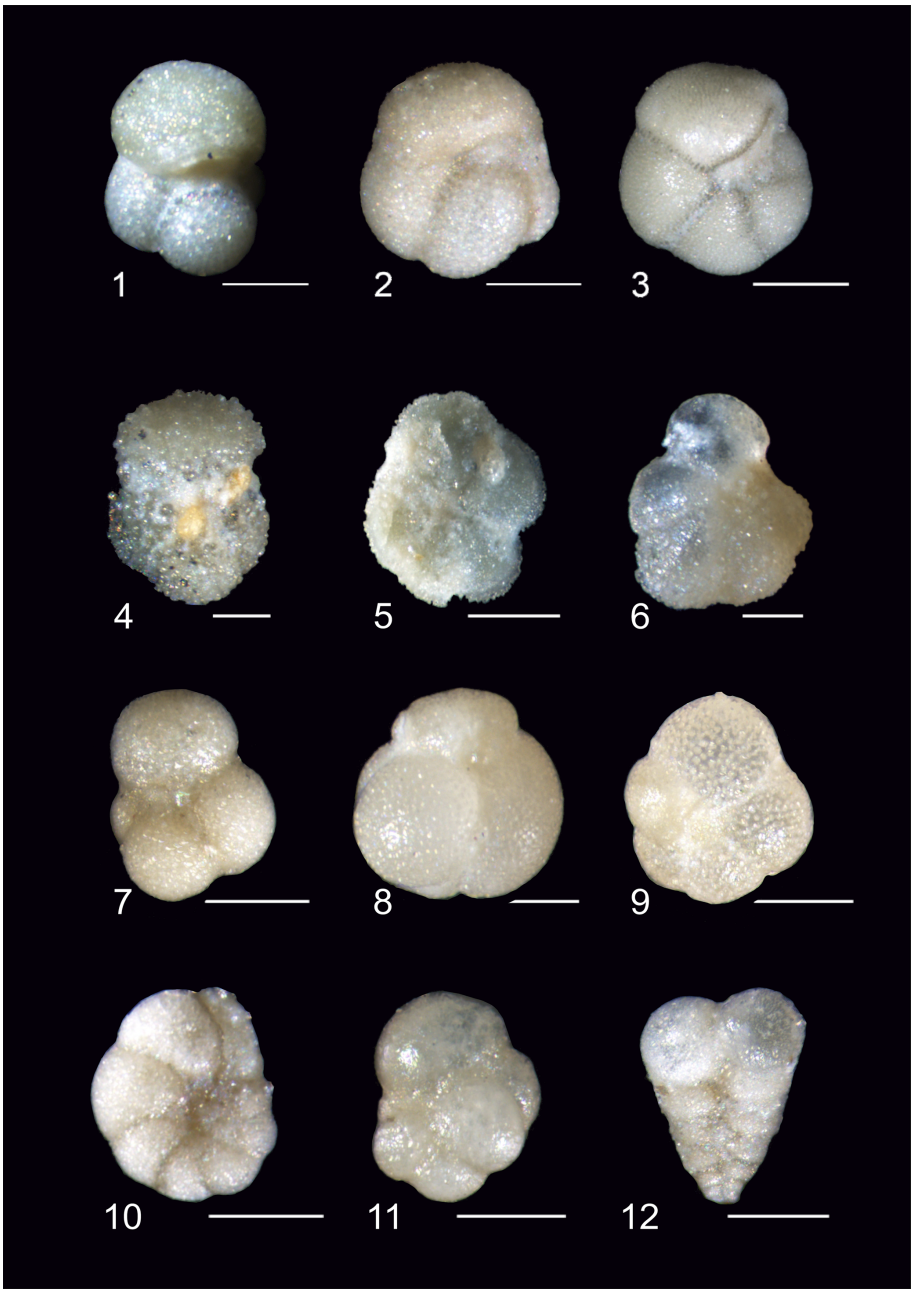


**Plate 5.** Z-stack images of planktonic foraminifera exhibiting general preservation characteristics of the Algodoal fauna. 1. *Turborotalita frontosa*. Zone E9, 5497 mbdt. 2. *Turborotalia pomeroli*. Zone E14, 5329 mbdt. 3. *Turborotalia cerroazulensis*. Zone E14, 5329 mbdt. 4. *Acarinina bullbrooki*. Zone E9, 5497 mbdt. 5. *Morozovelloides crassatus*. Zone E10, 5485 mbdt. 6. *Morozovelloides lehneri*. Zone E9, 5497 mbdt. 7. *Subbotina tecta*. Zones E16–O1, 5269 mbdt. 8. *Globigerinatheka kugleri*. Zone E10, 5473 mbdt. 9. *Globorotaloides suteri*. Zones E16–O1, 5269 mbdt. 10. *Pseudohastigerina micra*. Zones E16–O1, 5287 mbdt. 11. *Cassigerinella chipolensis*. Zones E16–O1, 5269 mbdt. 12. *Chiloguembelina ototara*. Zones E16–O1, 5269 mbdt. All scale bars are 100 µm.

sistent co-occurrence of *G. index* and rare *M. lehneri* down to 5485 mbdt, which both have their base within Zone E10 at 42.64 and 43.15 Ma, respectively; thus the Zone E9/E10 boundary occurs between 5485–5491 mbdt.

*Globigerinatheka kugleri*/*Morozovella aragonensis* Concurrent-range Zone (Zone E9), 43.26–43.88 Ma, 5491–5509 mbdt

The concurrent range of the nominate taxa between the Base of *Globigerinatheka kugleri* (∼ 43.88 Ma) and the Top of *Morozovella aragonensis* (43.26 Ma), a total of ∼ 18 m rep-

resenting Zone E9, was identified at the site, occurring from 5491–5509 mbdt. The top of this zone is identified between the Base of *G. index* (42.64 Ma) and the Base of *M. lehneri* (43.15 Ma) at 5485 mbdt and the Top of *M. aragonensis* (43.26 Ma) at 5491 mbdt. Available samples did not intercept the base of Zone E9 (∼ 43.88 Ma), with *G. kugleri* present through to the lowermost studied sample at 5509 mbdt.

### 3.3 Oceanicity/water depth

Oceanicity values (% planktonic foraminifera in the samples) remained relatively constant between 85 %–95 % throughout the sampling interval, indicating an oceanic setting with a palaeowater depth > 1000 m through 5491–5353 mbdt (Fig. 4a; following Hayward et al., 1999). Samples in the latest Eocene and through the EOT (5269–5311 mbdt) tended to have lower overall oceanicity values than earlier in the Eocene, possibly suggesting a minor reduction in local sea level to a sub-oceanic setting (< 1000 m b.s.l.; Fig. 4a).

### 3.4 Coarse fraction indicators

Weight % bulk sediment coarse fraction (> 63 µm) can indicate foraminiferal productivity (Luciani et al., 2017a), clay input/sediment dilution (Kelly, 2002), or carbonate dissolution (alongside current intensity; e.g. McCave, 2007), where dissolution often leads to fragmentation of foraminiferal shells and a decrease in the coarse sediment size fraction relative to bulk sediment weight (e.g. Broecker and Clark, 1999). Weight % coarse fraction values display high variability (∼ 25 %–65 %) throughout the Algodoal section (Fig. 4b), with peak values (∼ 67 %) immediately preceding the Eocene–Oligocene Boundary (EOB). The lowest coarse fraction values are found in the ORG-2 interval (24 %) at 5497 mbdt. However, we interpret these values with caution given the difficulties in consistently breaking down the sediment, with many still containing lumps of bulk sediment.

### 3.5 Absolute abundance of planktonic foraminifera

Absolute abundance of planktonic foraminifera in the samples was highly varied between 55 and 6781 *n*/g (Fig. 4c). Higher absolute abundances were present throughout the middle Eocene, with a peak value of 6781 *n*/g at 5491 mbdt succeeded by a steady decline in abundance throughout the remainder of the study interval reaching a low (55 *n*/g) in the latest Eocene and early Oligocene.

### 3.6 Diversity indices

Per-sample species richness varied between 44 and 61 species throughout the record (Fig. 4d; Table S4), with the highest values in the oldest Eocene sample within Zone E9 and then lower values fluctuating between 44 and 55 throughout the remainder of the Eocene. Species richness decreased across the EOB from ∼ 48–44 species, but values subsequently increased, reaching 54 species towards the top of Zone O1 with first appearances of more typical Oligocene species such as *Ciperoella ciperoensis*, *Dentoglobigerina sellii*, *Globigerinita glutinata*, *Paragloborotalia opima*, *Paragloborotalia pseudocontinuosa*, and multiple species of *Tenuitella*. Overall, Shannon's diversity index ($H'$) values increase through the Eocene and Oligocene, indicating an overall increase in assemblage evenness with diverse communities made up of similar numbers of individuals (Fig. 4e). This trend is interrupted by two distinct minima at 5479–5461 and 5293 mbdt in the middle Eocene (Zone E10) and earliest Oligocene (Zone O1), respectively, indicating reduced species richness and high species dominance (Fig. 4e).

### 3.7 Relative abundance of genera

The faunas encountered across the study interval at Algodoal are typical low-latitude assemblages (e.g. Wade and Pearson, 2008; Pearson and Wade, 2015), with the middle–late Eocene dominated by *Morozovelloides*, *Acarinina*, *Globigerinatheka*, *Turborotalia*, *Dentoglobigerina*, and *Subbotina*(Fig. 5). Hantkeninids, whilst never abundant, were present only sporadically through the study section, and, when present, they were poorly preserved at this site. Similarly to recent studies from other low-latitude sites (Aljahdali et al., 2020; Wade et al., 2021; Coxall et al., 2021), *Globoturborotalita* is a significant faunal constituent (up to 27 %) at Algodoal, perhaps indicating an ecological preference to certain middle–late Eocene tropical regions.

Middle Eocene assemblages are dominated by acarininids, specifically the small taxon *A. collactea*, constituting 16 %–28 % of the total assemblage from 5503–5461 mbdt, whilst typical larger tropical forms such as *Acarinina rohri* and *Acarinina topilensis* are also present (Berggren et al., 2006). Up-section, acarininids decrease in abundance throughout Zone E10 (5461–5401 mbdt) and are rare/absent within the succeeding samples. Samples from 5503–5401 mbdt exhibit relatively constant constituents of *Catapsydrax* (1 %–5 %), *Globigerinatheka* (1 %–3 %), *Morozovella*/*Morozovelloides* (6 %–9 %), *Subbotina* (3 %–8 %), *Globoturborotalita* (20 %–27 %), and *Pseudohastigerina* (2 %–5 %), with *Globoturborotalita* and *Pseudohastigerina* present continuously throughout the entirety of the study section (including in the > 63 µm fraction above 5311 mbdt) (Fig. 5). Through the whole section, *Globoturborotalita* and *Pseudohastigerina* exhibit relative abundance fluctuations between 8 %–27 % and 0.5 %–5 %, respectively. The sample from 5353 mbdt which marks the base of Zone E14 (∼ 38 Ma) shows distinct faunal disparity to the immediately adjacent samples, with an absence of large (> 125 µm) acarininids, morozovelloidids (excluding a single, poorly preserved *M. crassatus*), parasubbotinids, and planorotalitids. The relative abun-

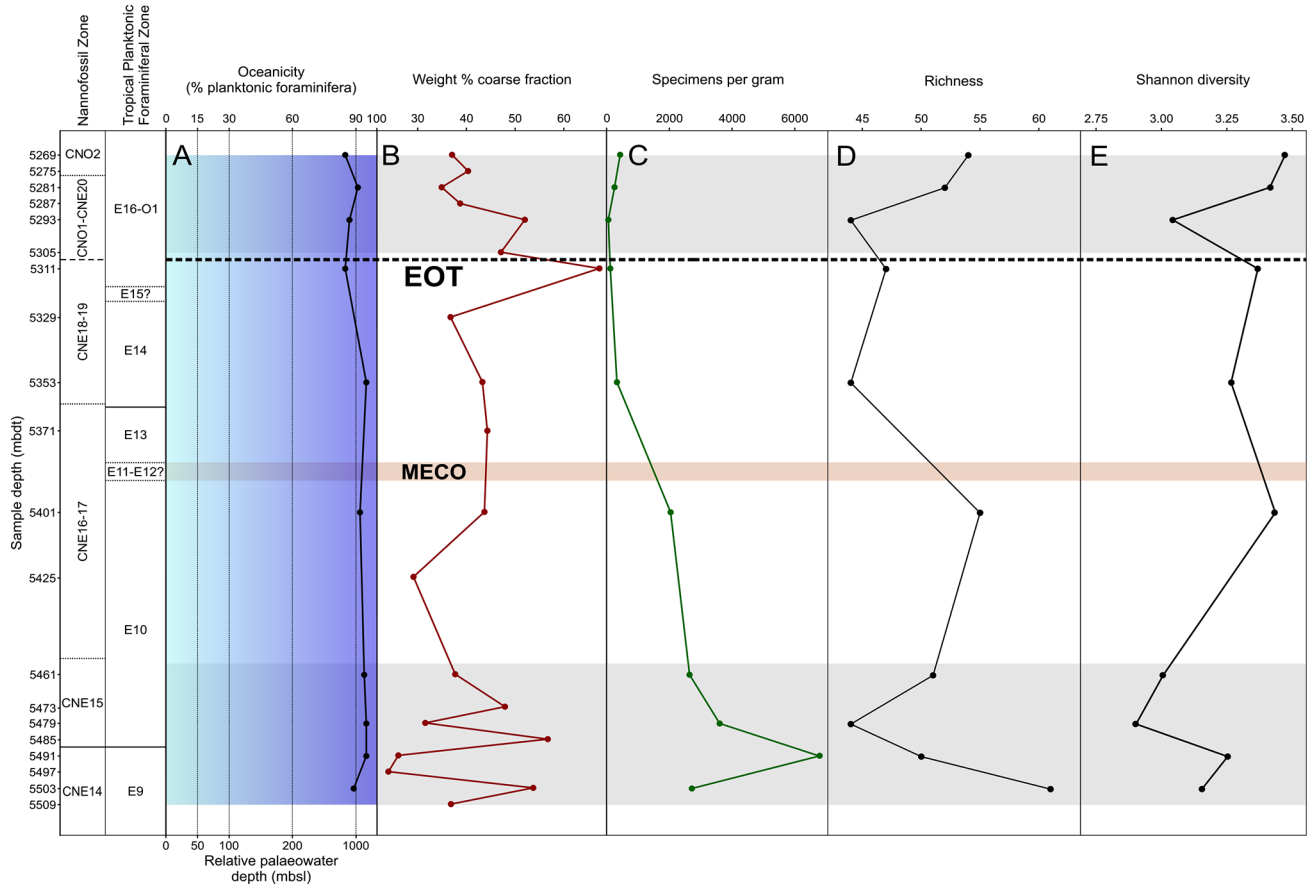


**Figure 4.** Middle Eocene–early Oligocene planktonic foraminiferal palaeoenvironmental and assemblage indicators in Algodoal. Calcareous nannofossil and planktonic foraminiferal biozonation with A, oceanicity (% planktonic foraminifera) values and relative palaeowater depth; B, weight % coarse fraction; C, number of foraminiferal specimens per gram of sediment; D, species richness; and E, Shannon diversity. Organic-rich intervals (ORG-1 and ORG-2) are shown by horizontal grey shaded intervals. The position of the EOT is approximated with a dashed line, and the Middle Eocene Climatic Optimum (MECO) duration is tentatively shown by the horizontal orange shaded interval.

dances of catapsydracids, globigerinathekids, turborotaliids, and subbotinids increase up-section from 5401 mbdt. The first (rare) occurrence of *Dentoglobigerina* is at 5401 mbdt, and they endure as a consistent (6 %–9 %) faunal component for the remainder of the studied interval. At 5311 mbdt, a notable shift in faunal character occurs, with the last occurrence of *Globigerinatheka*, the first appearance of *Cassigerinella*, and a considerable increase in *Chiloguembelina*, *Tenuitella*, and *Globorotaloides*, which all display reasonably high faunal representation (∼ 8 %). Congruently, *Subbotina* and *Turborotalia* show a general decline in relative abundance. The early Oligocene sample from 5293 mbdt shows a continued decline in the subbotinids, from a peak of 26 % at the Zone E13/14 boundary (5353 mbdt) to a low of 3 % by 5293 mbdt. Globoturborotalids and paragloborotalids display the inverse trend, increasing in abundance across the EOT, whilst the remainder of faunal constituents remain relatively unchanged. Further into the early Oligocene (5281–5269 mbdt) there is minor recovery of the subbotinids, increased dominance by *Tenuitella*, and general stabilization among most represented genera (Fig. 5).

### 3.8 Relative abundance and richness of ecogroups

During the middle Eocene (5503–5461 mbdt, zones E9 and E10), ecogroup 1 (symbiotic surface mixed layer – SML) species make up ∼ 50 %–60 % of the total fauna, ecogroups 2 and 3 (asymbiotic SML and thermocline, respectively) make up ∼ 10 %–30 % each, ecogroup 4 (sub-thermocline) makes up ∼ 8 %, and ecogroup 6 (upwelling/high productivity) makes up < 2 % (Fig. 6a). However, from 5461–5311 mbdt (zones E10–E16) there is a gradual turnover in ecogroup dominance, with a decline in ecogroup 1 from ∼ 60 % to 6 % and increases in ecogroups 2, 4, and 6 (to ∼ 30 %, 30 %, and 10 %, respectively; Fig. 6a). Ecogroup 3 shows minimal abundance change during the entire study section. During the Oligocene (5293–5269 mbdt), there were roughly equal proportions of all six ecogroups (Fig. 6a). There is a substantial decrease in the species richness found within ecogroup 1

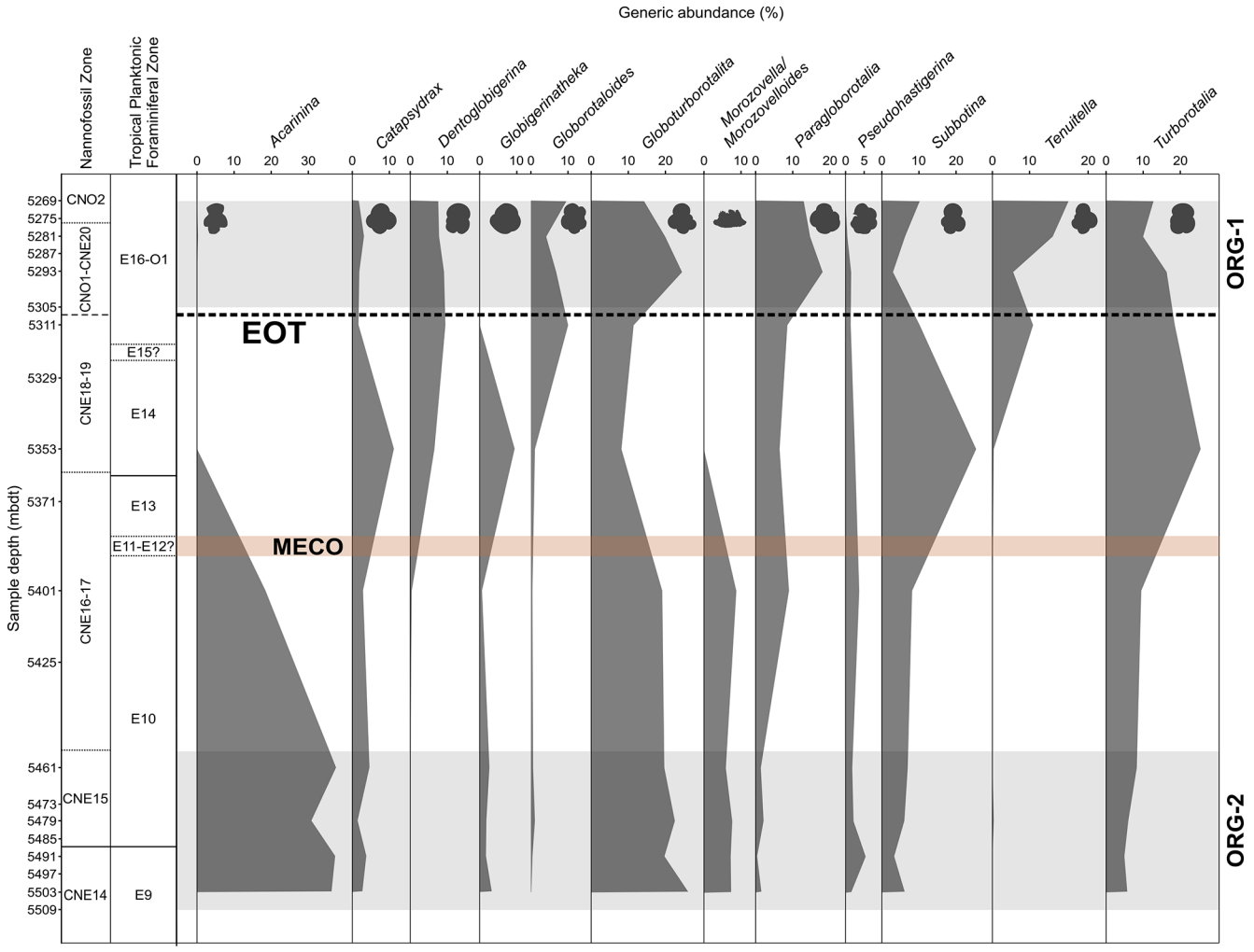


**Figure 5.** Middle Eocene–early Oligocene planktonic foraminiferal generic assemblage data in Algodoal Well. Calcareous nannofossil and planktonic foraminiferal biozonation and planktonic foraminiferal generic assemblage percentage data. Organic-rich intervals (ORG-1 and ORG-2) are highlighted by horizontal grey shaded intervals. The position of the EOT is approximated with a dashed line, and the Middle Eocene Climatic Optimum (MECO) duration is tentatively shown by the horizontal orange shaded interval.

from 5503–5353 mbdt (Zones E9–E14), with no recovery through the rest of the study section (Fig. 6b). Ecogroup 2 remains relatively stable throughout (Fig. 6c). Ecogroup 3 exhibits a slight increase in species richness at 5401 mbdt (Zone E10) before decreasing again and then showing rising species richness after the EOT from 5293–5269 mbdt (Zones E16–O1) (Fig. 6d). Both ecogroup 4 and ecogroup 6 show consistent increases in species richness from the base of the section upwards (Fig. 6e and f).

### 3.9 Statistical analysis

Cluster analysis through mean linkage (UPGMA) was performed simultaneously with correspondence analysis at species level and reveals consistent clustering of discrete sample suites representing the EOT–early Oligocene interval (5269–5311 mbdt; Group I) and the middle Eocene (5401–5503 mbdt; Group II) (Fig. 7). Notably, the interim middle–late Eocene-aged sample at 5353 mbdt was consistently separated from these two clusters but with more similarity to the EOT–early Oligocene samples. Correspondence analysis displayed good ordering within sample depth from shallow to deep ranking right–left. Bray–Curtis distance was employed to determine the relationship between species composition of sample depths, wherein final distance is more influenced by species dominance (Faith et al., 1987). Both measures revealed separation of each cluster into discrete stratigraphically constrained "sub-clusters" with the exclusion of the sample from 5353 mbdt (∼ 38 Ma), which showed more similarities with cluster I.

The primary factor in the separation of the two statistical sample clusters (Fig. 7) is likely the relative prevalence of *A. collactea* and *P. nana* within the middle Eocene and

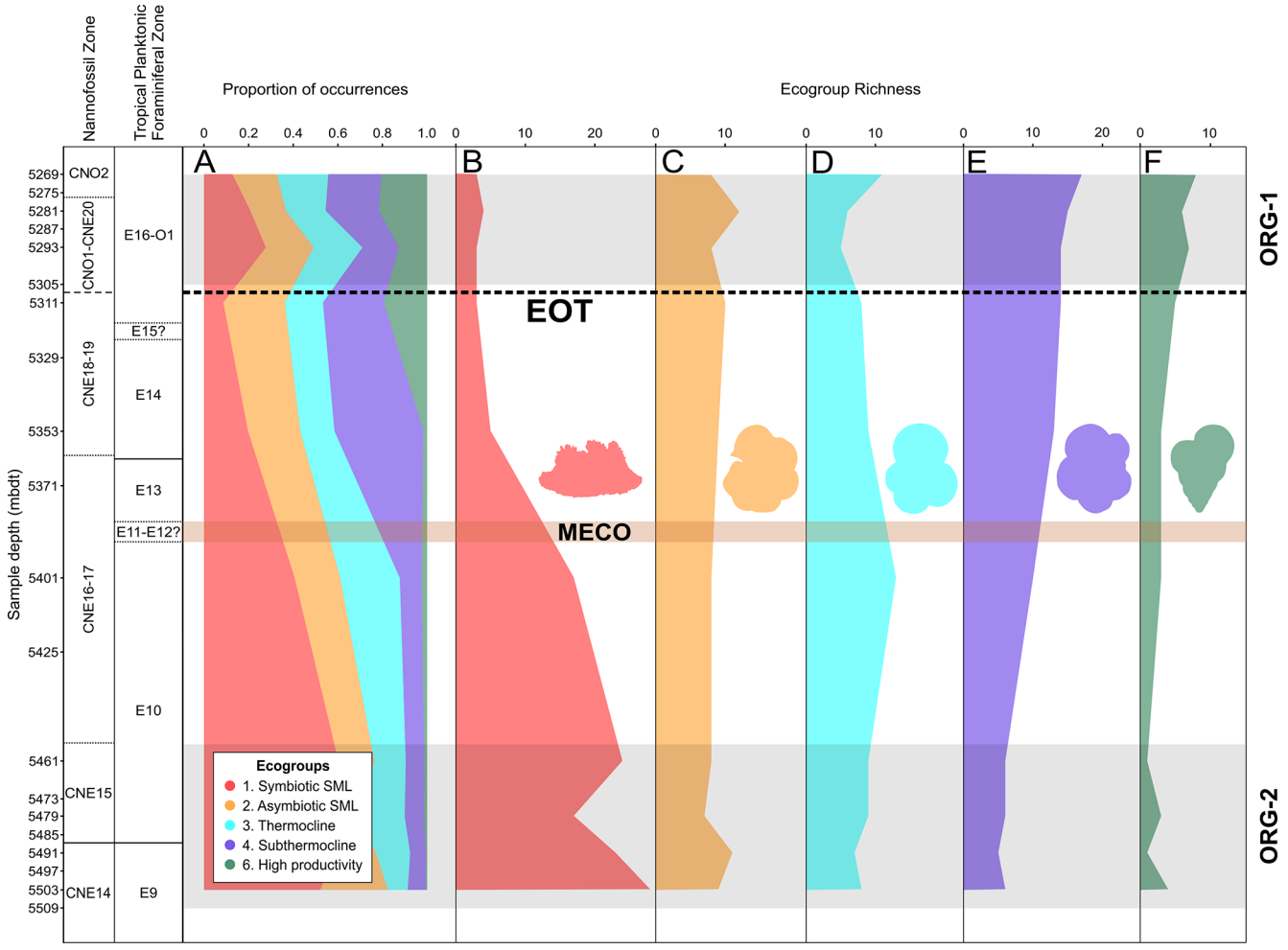


**Figure 6.** Middle Eocene–early Oligocene planktonic foraminiferal ecogroup assemblage data in Algodoal Well. Calcareous nannofossil and planktonic foraminiferal biozonation, ecogroup assemblage proportions (A), and ecogroup richness (B–F). Organic-rich intervals (ORG-1 and ORG-2) are highlighted by horizontal grey shaded intervals. The position of the EOT is approximated with a dashed line, and the Middle Eocene Climatic Optimum (MECO) duration is tentatively shown by the horizontal orange shaded interval. Ecogroup 1 = open-ocean mixed layer tropical/subtropical, with symbionts; ecogroup 2 = open-ocean mixed layer tropical/subtropical, without symbionts; ecogroup 3 = open-ocean thermocline; ecogroup 4 = open-ocean sub-thermocline; ecogroup 6 = upwelling/high productivity.

EOT–early Oligocene samples, respectively (Fig. 5; see Table S4). Moreover, the consistent exclusion of the sample at 5353 mbdt from the clusters is likely attributable to this sample having a faunal composition intermediate between both clusters, along with a distinct abundance of *Subbotina* and *Turborotalia*. The Bray–Curtis similarity measure divided the primary clusters into discrete pairings of adjacent stratigraphic horizons, reflecting their similar assemblage composition. This suggests that a good level of assemblage similarity was maintained within successive stratigraphic levels on either side of the sample at 5353 mbdt.

## 4 Discussion

### 4.1 Biostratigraphic utility of planktonic foraminifera within Algodoal

The planktonic foraminiferal biostratigraphy of Algodoal is generally consistent with the tropical/subtropical biozonation schemes of Wade et al. (2011). Zones E9, E10, E11–13, E14, and E16–O1 were identified, depicting assemblages and marker species generally consistent within low-latitude studies. However, the lack or rarity of some key primary markers, e.g. *Hantkenina* or *O. beckmanni*, hindered the differentiation of some zones; thus, secondary markers were frequently employed to infer zonal boundaries, though they were left undifferentiated (Fig. 4).

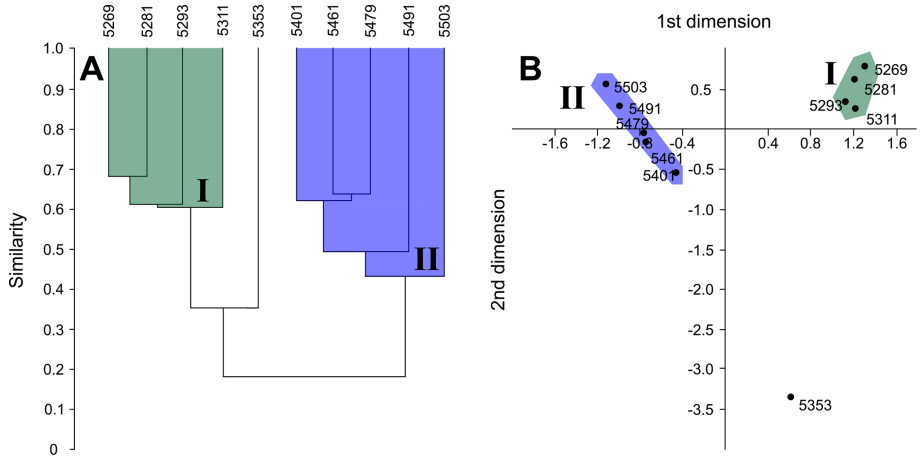


**Figure 7.** Middle Eocene–early Oligocene planktonic foraminiferal cluster and correspondence analysis results within Algodoal. A = Bray–Curtis similarity measure; B = correspondence analysis. Group I = EOT–early Oligocene; Group II = middle–late Eocene.

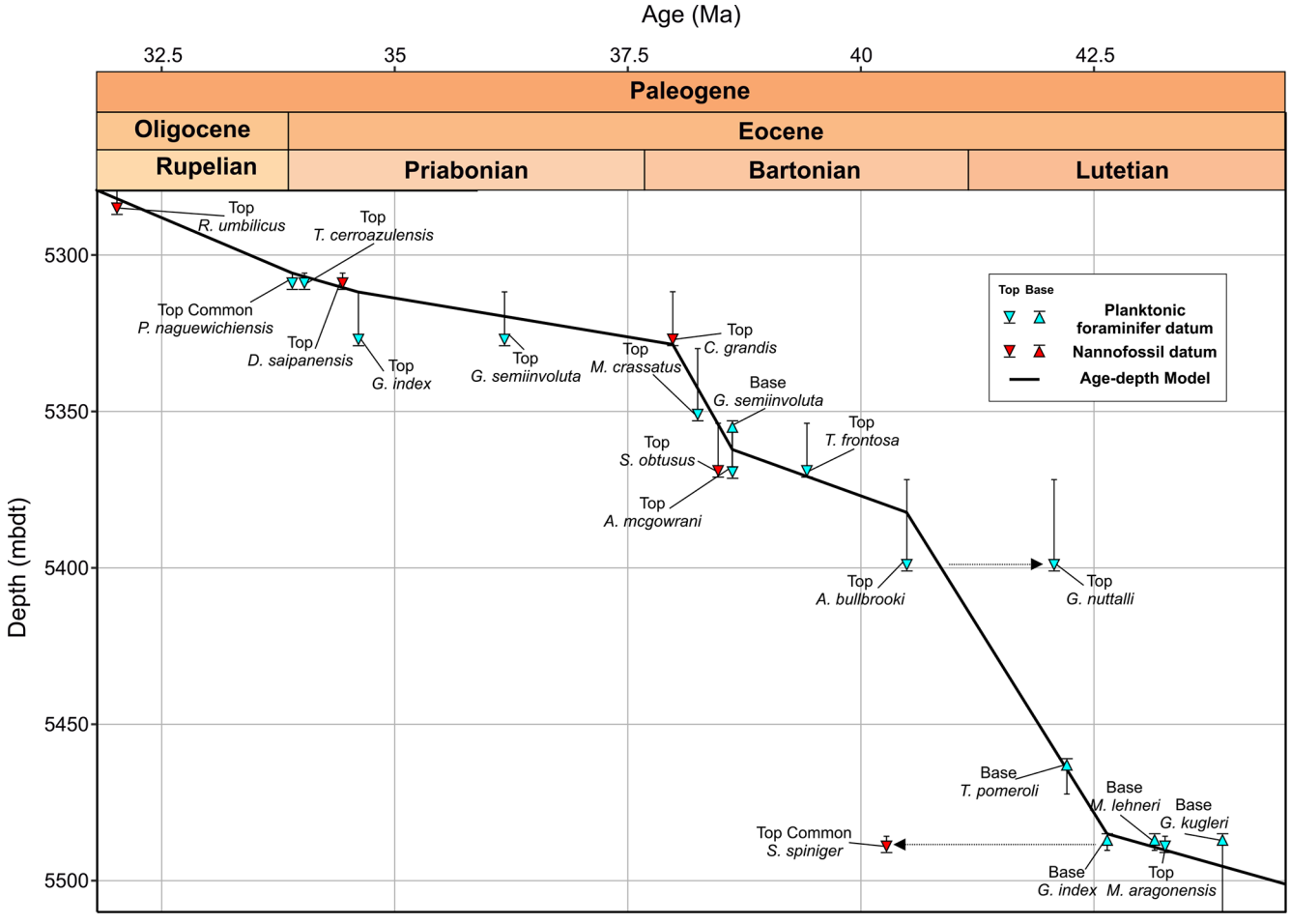


**Figure 8.** Middle Eocene–early Oligocene age–depth plot with planktonic foraminiferal (PF) and calcareous nannofossil (CN) datums from Algodoal. Both primary and secondary planktonic foraminifera datum ages are shown from the Geological Time Scale 2012 (Anthonissen and Ogg, 2012; Gradstein et al., 2012; Vandenberghe et al., 2012) and references therein, and calcareous nannofossil datum ages are from Fornaciari et al. (2010) and Agnini et al. (2014). Dashed arrows highlight datums which deviate from the age model (see text for discussion). Thin grid lines indicate age and depth increments.

Comparison of Algodoal planktonic foraminiferal biostratigraphy with wellsite calcareous nannoplankton biostratigraphy (Varol, 2004) updated to the Geological Time Scale 2012 (Anthonissen and Ogg, 2012; Gradstein et al., 2012; Vandenberghe et al., 2012) indicates generally good agreement above ∼ 5370 mbdt in the late middle Eocene to early Oligocene, where both groups suggest sedimentation rates ∼ 10 m Myr$^{-1}$ down to ∼ 5330 mbdt and an increase in rates to ∼ 44 m Myr$^{-1}$ between ∼ 5330 and ∼ 5370 mbdt (Figs. 3 and 8; Table 2). However, below ∼ 5370 mbdt, planktonic foraminifera indicate an increase in sedimentation rates to ∼ 20 m Myr$^{-1}$, with the exception of the Top of *G. nuttalli* (∼ 42.07 Ma) at 5401 mbdt (Fig. 8). We note that specimens attributed to *G. nuttalli* occur sporadically into zones E13 and E14 within the equatorial Pacific ODP Site 865 and the Alano section in northern Italy (Agnini et al., 2011; Edgar et al., 2020). On the other hand, for calcareous nannoplankton, the highest common occurrence of *Sphenolithus spiniger* (40.27 Ma) at 5491 mbdt suggests an increase in sedimentation rates to ∼ 50 m Myr$^{-1}$, placing the interval ∼ 2–3 million years younger than planktonic foraminiferal datums (Fig. 8). This is possibly due to this datum being more consistent for mid-latitudes (Fornaciari et al., 2010), though reworking (natural and/or drilling-induced) cannot be ruled out, where possible reworking of *M. crassatus* was observed up-section. Another possible scenario may be ecological factors such as delayed dispersion and/or extirpation within these species (see Brombacher et al., 2021; Lam et al., 2022; Niederbockstruck et al., 2024). Furthermore, some planktonic foraminiferal biostratigraphic markers, such as the Base of *G. index* (42.64 Ma) and the Base of *M. lehneri* (43.15 Ma), were observed at the same depth (5485 mbdt). This discrepancy in *G. index* was also noted at the low-latitude NKK-1 site in Java, Indonesia (Coxall et al., 2021), suggesting regional ecological/biogeographic mechanisms may be at play or that this may simply be due to borehole mixing in the case of the Algodoal Well (Bown et al., 2022). This warrants further study of low-latitude sites covering the same temporal interval to determine if any such offsets are longitudinally diachronous.

### 4.2 Ecogroup and generic dynamics

Ecogroup richness (species richness within each ecogroup) and assemblage composition in the Algodoal Well (Figs. 5 and 6) showed decreasing abundances of symbiotic SML (ecogroup 1) and increasing open-ocean thermocline and sub-thermocline dwellers (ecogroups 4 and 6). Global records assembled from the Triton database (Fenton et al., 2021) show similar patterns to those at Algodoal (Fig. 9). Prior to the Middle Eocene Climatic Optimum (MECO; ∼ 40 Ma), the assemblage was dominated by ecogroup 1, which comprised ∼ 50 % of the global fauna. Here, ecogroups 2, 3, and 4 made up ∼ 15 %–20 % each, whilst ecogroup 6 was rare, ∼ 1 %–5 %. Between the MECO and the EOT, the same turnover documented in Algodoal is seen on the global stage (Figs. 6 and 9), where a new stable regime is established in the early Oligocene, with ecogroup 1 reduced to ∼ 5 %–10 % of the total assemblage and ecogroup 4 increased to 40 %–50 %. Furthermore, global patterns for ecogroup 6 also followed those seen in Algodoal, increasing to represent ∼ 10 % of the global assemblage (Fig. 9). Amongst ecogroups 2 and 3, similar patterns of consistency were exhibited, though ecogroup 3 became more established globally, as opposed to ecogroup 2 at Algodoal. These ecogroup changes are consistent with global cooling and changes in trophic levels of the surface ocean associated with physical and thermal niche restructuring of the western Atlantic and global ocean post-MECO (Wade and Pearson, 2008; Katz et al., 2011; Lowery et al., 2020; Yasuhara and Deutsch, 2023; Swain et al., 2024).

At Algodoal, in the middle Eocene (zones E9 and E10; 5503–5401 mbdt), ecogroup 1 is primarily composed of the muricate acarininids and muricocarinate morozovelloidids, along with a notable component of spinose, globular globoturborotalids, similar in character to the low-latitude Javan assemblages (Coxall et al., 2021). The latter make up a consistent proportion of ecogroup 1 for the entire study section and appears unaffected by global environmental perturbations, e.g. EOT or MECO (Figs. 5 and 6). We therefore suggest that the small size and consistent population of Eocene–Oligocene globoturborotalids in Algodoal likely indicates that they are ecologically flexible *r*-strategists (Hallock, 1985; Boersma and Premoli Silva, 1991), supported by their cosmopolitan biogeography (Olsson et al., 2006; Spezzaferri et al., 2018; Coxall et al., 2021).

Muricate and muricocarinate symbiont-bearers thrived within the (sub)tropical oligotrophic mixed-layer habitats of the late Palaeocene and the early and middle Eocene (Boersma et al., 1987; Pearson et al., 2001; Wade, 2004; Edgar et al., 2013, 2015; Swain et al., 2024). However, the morozovellids underwent a substantial abundance crash during the EECO, likely due to a combination of sustained temperature and ocean acidity increases causing algal photosymbiont bleaching from which they never recovered (Luciani et al., 2016, 2017a, b, 2021; D'Onofrio et al., 2020; Filippi et al., 2024), although this morphological and ecological niche was later filled by *Morozovelloides* (Aze et al., 2011). This gradual decline and eventual extinction of the muricate forms (*Morozovelloides* and large *Acarinina*) in the late middle Eocene, and the associated biotic turnover amongst planktonic foraminifera lineages and ecologies, is often attributed to palaeoceanographic changes associated with early cryosphere development (Keller, 1983; Boersma and Premoli Silva, 1991; Keller et al., 1992; Wade et al., 2008; Swain et al., 2024). Despite abiotic forces being the primary extinction driver amongst macroperforate planktonic foraminifera (Ezard et al., 2011; Lowery et al., 2020), Wade (2004) demonstrated that lowered sea surface temperatures alone were likely an insufficient trigger for these extinctions and instead proposed a combination of forcing factors

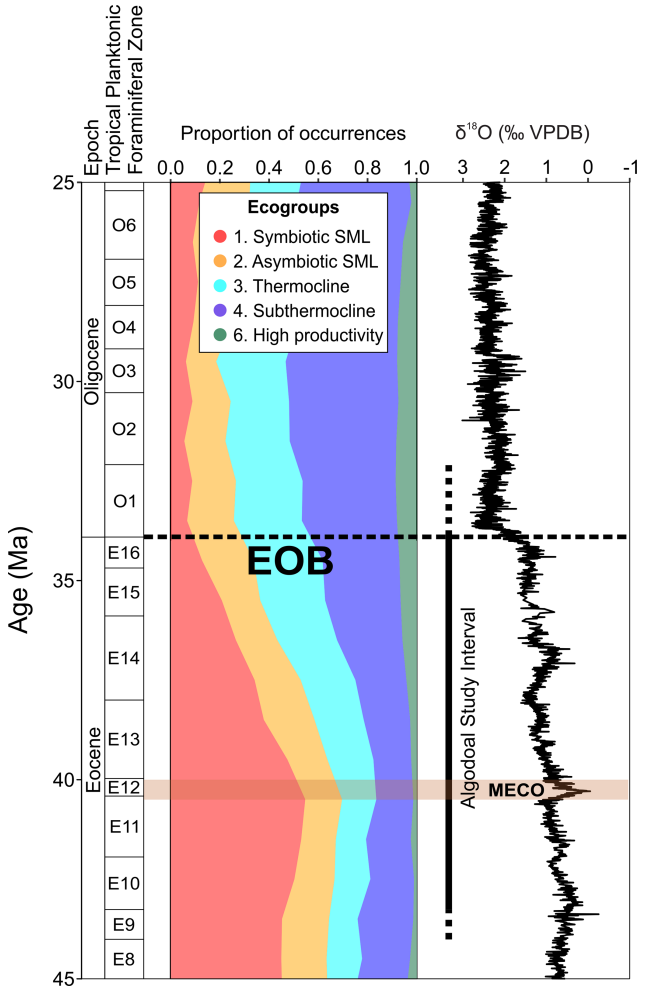


**Figure 9.** Middle Eocene–middle Oligocene planktonic foraminiferal ecogroup assemblage data from Triton (Fenton et al., 2021). Planktonic foraminiferal biozonation, ecogroup assemblage proportions, and benthic foraminiferal $\delta^{18}O$ data from Westerhold et al. (2020) with the Algodoal study interval are highlighted. Note that ecogroup 5 (high-latitude forms) is excluded from this plot. The position of the EOB is indicated with a dashed line, and the Middle Eocene Climatic Optimum (MECO) duration is shown by the horizontal orange shaded interval.

involving declining sea surface temperatures, niche elimination/trophic resource collapse, and a loss of symbiotic relationships (Wade et al., 2008; Wade and Olsson, 2009).

Within the Algodoal Well, biotic turnover of *Morozovelloides* and large *Acarinina* occurs between 5461 and 5311 mbdt in the late middle and late Eocene. Edgar et al. (2013) noted that despite the larger acarininids, morozovelloidids, and globigerinathekids all being assigned to ecogroup 1, they all exhibited different responses to the same environmental perturbation (MECO), indicating subtly different affinities/niches. However, the morozovelloidids ultimately died out within ∼ 11 kyr of the large acarininids (Wade et al., 2012), suggesting reduced sensitivity to the ongoing environmental stressors amongst globigerinathekids relative to the muricate forms, potentially a consequence of genus-specific ecological or morphological habits despite their similar niche occupation.

The muricate taxa (*Acarinina*, *Morozovella*, *Morozovelloides*, and *Igorina*) occupied an ecological habit analogous to that of modern spinose taxa, in warm, shallow oligotrophic waters (Douglas and Savin, 1978; Boersma et al., 1987; Pearson et al., 1993, 2022; D'Hondt et al., 1994; Norris, 1996). They yield amongst the most positive $\delta^{13}C$ values in the foraminiferal assemblage, indicative of habitation of the uppermost water column with algal photosymbionts (Pearson et al., 1993; Wade, 2004; Berggren et al., 2006; Pearson and Berggren, 2006; Sexton et al., 2006b; Wade et al., 2008; John et al., 2013; Edgar et al., 2015, 2017; Luciani et al., 2017a, b). The globigerinathekids, on the other hand, also inferred to have hosted algal symbionts, exhibit stable isotopic values indicating slightly deeper niche occupation, perhaps within the lower mixed layer or uppermost thermocline (Wade, 2004; Premoli Silva et al., 2006; Sexton et al., 2006b; John et al., 2013; Edgar et al., 2015, 2017; Anagnostou et al., 2016). As well as a slightly deeper habitat, globigerinathekid morphology may have played a significant role in their survival when the corresponding muricates became extinct. Sinking velocity experiments on modern planktonic foraminifera reveal that spherical morphogroups (e.g. *Orbulina universa*) experience more drag within the water column than their non-spherical counterparts (McNown and Malaika, 1950; Walker, 2019). Furthermore, seawater viscosity is primarily a factor of temperature in the open ocean (Defant, 1961), where viscosity decreases rapidly with increasing water temperature, offering less resistance to sinking particles (Fofonoff, 1962; Leckie, 1989). Therefore, a spherical morphology may have ecologically preconditioned *Globigerinatheka* to succeed where the muricates failed. Globigerinathekid shape and higher drag coefficient may have permitted adaptive habitat migration (e.g. Woodhouse et al., 2021) or potentially limited disruption to their vertical migration during gametogenesis and spine-shedding, which may have affected other morphologies. Indeed, despite the eventual extinction of *Globigerinatheka* in the latest Eocene, the ability of spherical morphotypes to endure intervals of global physical and trophic alteration of the oceans is evidenced by the evolution of both *Orbulinoides beckmanni* during the MECO (Edgar et al., 2010, 2020) and *Orbulina universa* during the Miocene Climatic Optimum (17–14.8 Ma), where the latter underwent subsequent proliferation throughout the global ocean (Schiebel and Hemleben, 2017; Boscolo-Galazzo et al., 2021, 2022). Ultimately, the protracted sea surface temperature increases associated with the MECO (∼ 40 Ma), succeeded by continued global cooling, were likely compounded by physical and trophic changes in the vertical character of the water column that collectively contributed to the extinction of the large muricate/muricoarinate forms ∼ 38 Ma (Wade, 2004; Luciani et al., 2010; Arimoto et al.,

2020; Kearns et al., 2021, 2023). Eventually, despite outlasting the larger acarininids and morozovelloidids, continued environmental changes appear to have ultimately led to the extinction of *Globigerinatheka* in the latest Eocene, following which symbiotic SML dwellers were largely absent from the oceans until the mid-Miocene (Wade, 2004, Boscolo-Galazzo et al., 2021, 2022).

Following the MECO, improved habitability and exploitation of deeper waters is evidenced by an increase in richness and assemblage dominance by ecogroup 4 (sub-thermocline) catapsydracids and subbotinids within Algodoal and across the globe (Figs. 5, 6 and 9). Overall, ecogroup turnover supports a reduction in global temperature and strengthening latitudinal temperature gradients (Schmidt et al., 2004a, b; Cramer et al., 2009, 2011; McGowran, 2012; Inglis et al., 2015; Gaskell et al., 2022; Swain et al., 2024) but also suggests that the improving efficiency of the biological carbon pump exporting more particular organic matter deeper is likely linked to the onset of middle–late Eocene cooling (John et al., 2013; Jones et al., 2019). This mechanism is similar to that following the middle Miocene (Boersma and Premoli Silva, 1991; Ezard et al., 2011; Boscolo-Galazzo et al., 2021, 2022; Woodhouse et al., 2023b). Ecogroup trends documented within Algodoal and globally (via Triton) suggest a gradual ecological turnover after the MECO culminating at the EOT. The taxa lost at the EOT (e.g. hantkeninids, turborotalid species) were subject to $\sim$ 6 million years of decreasing global temperatures yet were unable to survive this transient cooling event. Perhaps evolving in a greenhouse world had funnelled many of these taxa into troughs of their respective evolutionary adaptive landscapes that were incompatible with an environmental threshold surpassed by the advent of the icehouse climate state (Coxall and Pearson, 2007).

Early Oligocene assemblages at Algodoal have relatively low $H'$ values, a typical indicator of biotic stress and ecological disturbance also found in the Tanzanian EOT record (Wade and Pearson, 2008), and ecogroups 1 and 3 show continued species loss (Fig. 6). All genera within these two ecogroups suffered distinct richness losses, with the exclusion of the primary faunal constituents, the globoturborotalids and paragloborotalids. The end result is a regime shift within assemblages to one dominated by spinose, globular thermocline dwellers, particularly the paragloborotalids, e.g. *Paragloborotalia nana*, and a reduction in the abundance and diversity of spinose subbotinids within the early Oligocene (Fig. 5). Shared morphological and ecological characters may suggest that an ecologically driven population control mechanism might have affected both genera similarly. Thus, changes to thermocline structure within the early Oligocene (e.g. Boersma and Premoli Silva, 1991; Wade and Pearson, 2008; Katz et al., 2011; Erhardt et al., 2013; Moore et al., 2014) may have led to trophic changes better suited to *Paragloborotalia*, which exhibit heightened speciation throughout the Oligocene, where they were abundant in eutrophic environments (Leckie et al., 2018). Additionally, the success and expansion of the paragloborotaliids may have led to niche competition with the remaining thermocline-dwelling subbotinids that had dominated the middle Eocene through high ecological niche plasticity (Kearns et al., 2021, 2023). The consistent abundance of paragloborotalids through the late Eocene–early Oligocene was also observed in Java (Coxall et al., 2021); however, they appear to be absent from the Tanzanian records (Wade and Pearson, 2008), despite the similar water depth of the latter to Algodoal. An abiotically driven ecological niche gradient amongst low-latitude sites may therefore have been governing the regional success of *Paragloborotalia*, perhaps also facilitating the opposing abundance trends amongst Hantkeninidae and *Paragloborotalia* observed between Algodoal and Tanzania (see below).

Early Oligocene samples above 5293 mbdt show re-establishment of an ecogroup and faunal distribution like those at 5311 mbdt, along with a marked increase within thermocline dweller diversity consistent with observations from Tanzania (Wade and Pearson, 2008). This suggests potential recovery and diversification amongst forms which survived the EOT in the newly established water column profile of the Oligocene, though the presence of forms exhibiting abnormalities within this interval (Plate 3) indicates ecological stress persisted following the EOT (e.g. Luciani et al., 2010). Similar occurrences of atypical morphologies are seen in Tanzanian and Javan low-latitude EOT sections (Wade and Pearson, 2008; Pearson and Wade, 2015; Coxall et al., 2021).

Hantkeninidae assemblages at Algodoal are more like relatively shallow-water Gulf Coast sites, where they are also very low and sporadic in abundance during the middle–late Eocene (e.g. Fluegeman, 1996; Miller et al., 2008; Fluegeman et al., 2009). In contrast, at most deep-sea sites (including ODP Leg 154, $\sim$ 3000 m b.s.l., $\sim$ 500 km northeast of Algodoal; see Fig. 2), Hantkeninidae are a rare but consistent enough component for biostratigraphy (Edgar et al., 2020; Coxall et al., 2000). Late Eocene forms *Hantkenina alabamensis* and *Cribrohantkenina inflata* are surface dwellers commonly found in shallower habitats than deeper (sub-)thermocline-dwelling early and middle Eocene forms (Coxall, 2000; Coxall and Pearson, 2006; Coxall et al., 2000, 2003). Despite the shallower water depth at Algodoal than at Ceara Rise, the lack of Hantkeninidae at Algodoal suggests an additional abiotic factor may be suppressing the local population, supported by consistent and abundant hantkeninid assemblages across other important low-latitude shallow-water sites (Coxall et al., 2021) and similar water depth sites (Wade and Pearson, 2008; Pearson and Wade, 2015). We suggest that their rarity may relate to the proximity to the proto-Amazon River mouth creating trophic conditions detrimental to their life strategy, and this is supported by the increasing ecogroup 6 (upwelling/high productivity) species, which suggests a possible upper productivity limit for late Eocene forms within the lineage (see discussion below).

### 4.3 Organic-rich intervals: dissolution indices and foraminiferal composition

Organic-rich intervals (ORG-1 and ORG-2 in the EOT–early Oligocene and early middle Eocene, respectively) at Algodoal are coincident with changes in faunal signals and foraminiferal preservation, suggesting increased water column productivity and thus organic matter flux to the sea floor. Weight % coarse fraction and $P/B$ ratios (% oceanicity, Fig. 4) can be indicators of dissolution; however, they show only a weak relationship ($r^2 = 0.43908$, $p < 0.05$), indicating that dissolution may not be the dominant control on these records. Indeed, we do not see extensive evidence of dissolution on foraminiferal shells. Furthermore, foraminiferal preservation and weight % coarse fraction also show some correlation ($r^2 = 0.38091$, $p < 0.01$), within which lower weight % coarse fractions values tended to correspond to higher-quality preservation, in contradiction with observations of organic-rich intervals elsewhere, e.g. across the MECO of NE Italy (Luciani et al., 2010) and Mesozoic Ocean Anoxic Events (Jones et al., 2023).

The tectonic and palaeoceanographic conditions that contributed to decreasing atmospheric $CO_2$ concentrations at the EOT (Kennett et al., 1975; Pearson et al., 2009; Zhang et al., 2013; Anagnosotu et al., 2016; Foster et al., 2017; Houben et al., 2019; Rae et al., 2021; Rodrigues de Faria et al., 2024) facilitated deepening of the calcium carbonate compensation depth (CCD; van Andel and Moore, 1974; Griffith et al., 2011; Pälike et al., 2012; Wade et al., 2020). However, coarse fraction values within ORG-1 are inconsistent with this hypothesis, decreasing in value across and after the EOT, which may suggest local CCD and lysocline shoaling in the equatorial Atlantic. However, $P/B$ ratios also decrease, indicating a switch from oceanic to sub-oceanic conditions and a slightly shallower water setting at Algodoal (Fig. 4), likely related to the global $\sim$ 50–70 m sea level drop associated with rapid expansion of the East Antarctic Ice Sheet at this time (Miller et al., 2008; Miller et al., 2020; de Lira Mota et al., 2023). These two observations can be reconciled because even a minor sea level fall would lead to a setting more proximal to the South American mainland increasing run-off and thus sediment contribution (e.g. de Lira Mota et al., 2023). This is supported by the gradual decline in the number of specimens per gram of sediment through the study section, with minimum values in the earliest Oligocene (Fig. 4). Unfortunately, the resolution, lack of primary marker species, and extent of our age model do not allow us to determine if sedimentation rates increased in the early Oligocene (Figs. 3 and 8). During this time, closer proximity to the coastline, coupled with uplift within the Eastern Cordillera (Gómez et al., 2003; Parra et al., 2005; Bayona et al., 2008; Mora et al., 2010) and downcutting of proto-Amazonian tributaries, may have increased terrestrial run-off in the Foz do Amazonas Basin. Model–data comparisons of Amazonia across the EOT also indicate a reduction in regional seasonality with strengthened precipitation, possibly altering the basinal hydrology and weathering regime (Antoine et al., 2021; Toumoulin et al., 2022). Furthermore, there is evidence for proto-Atlantic Meridional Overturning Circulation (AMOC) from middle Eocene deep-sea deposits (Hohbein et al., 2012; Boyle et al., 2017), with proto-AMOC intensification across the EOT (Katz et al., 2011; Borrelli et al., 2014; Coxall et al., 2018; Hutchinson et al., 2019, 2021). An evolving proto-AMOC would have altered Atlantic Ocean salinity, circulation, and possibly the Intertropical Convergence Zone, contributing to observed changing precipitation patterns (Antoine et al., 2021). Enhanced run-off would likely cause an increase in nutrient availability of surface waters, which may have been exacerbated regionally and globally due to the input of Subantarctic Mode Waters from the Southern Ocean as the Antarctic ice sheet expanded, contributing to upwelling of nutrients along continental margins and low-latitude nutrient leakage (Boersma and Premoli Silva, 1991; Zachos et al., 2001; Egan et al., 2013; Jones et al., 2019). Indeed, this is evidenced by a global influx of high-productivity/upwelling (ecogroup 6) taxa following the MECO (Fig. 9) in Triton and by an increase in biserial *Chiloguembelina* and *Streptochilus* at Algodoal (Fig. 6), indicators of heightened productivity and/or dysoxia (Boersma and Premoli Silva, 1986, 1989; Boersma et al., 1987; Leckie et al., 1998; Smart and Thomas, 2006; King and Wade, 2017; Bryant et al., 2021).

Higher productivity coupled with expansion of the oxygen minimum zone (OMZ) could have also prompted increased production and preservation of organic matter (Figs. 4–6). Reduced oxygen levels would trigger a localized reduction in seawater/pore water pH (Luciani et al., 2010) and increased carbonate dissolution within ORG-1, also consistent with lower absolute foraminiferal abundances and a higher proportion of benthic relative to planktonic foraminifera, the former being more resistant to dissolution (Hancock and Dickens, 2005). However, planktonic foraminiferal preservation was best within this section, and increased run-off may have contributed to rapid burial permitting a higher degree of preservation potential within the early Oligocene (Bown et al., 2008). Future work on the benthic foraminiferal faunas may help resolve bottom-water conditions and changes in seafloor oxygenation.

A different faunal composition of ecogroup 6 forms is observed in the older ORG-2 (5461–5503 mbdt) than that in ORG-1 (Figs. 5 and 6). In ORG-2, ecogroup 6 includes *Paragloborotalia griffinae*, *Paragloborotalia inaequispira*, and *Pseudoglobigerinella bolivariana*, all of which became extinct prior to ORG-1. In contrast, ORG-1 is characterized by a dominance of biserial forms that are rare or absent in ORG-2. Both intervals indicate elevated productivity, with ORG-2 also having high absolute foraminiferal abundance values. Nevertheless, the lack of biserial taxa in ORG-2 may suggest that there are nuanced differences in palaeoceanographic conditions and/or biserial ecological habits.

Despite the ecogroups of Aze et al. (2011) being assigned to only macroperforate taxa, Luciani et al. (2010) documented the macroperforate *Pseudohastigerina* (ecogroup 2; Aze et al., 2011) alongside the microperforate *Streptochilus* and *Chiloguembelina* as all having a low-oxygen-tolerant generalist/opportunist life strategy. At Algodoal, the pseudohastigerinids have notably heightened abundance within ORG-2 and at 5401 mbdt outside the organic-rich interval (Fig. 5). The species present in this study, *Pseudohastigerina micra*, *Chiloguembelina ototara*, and *Streptochilus martini*, are also known through stable isotope data (Poore and Matthews, 1984; Boersma et al., 1987; Pearson et al., 2001, 2018; Barrera and Huber, 1991; Sexton et al., 2006b; Wade and Pearson, 2008; Olsson and Hemleben, 2006; Wade and Cheng, 2024) to have occupied similar depth habits within the thermocline. However, despite these similarities, upon observation of assemblage dynamics across the entire study section, they have almost contrasting abundances. This may be a closed-sum effect or may indicate interspecific competition (Fig. 5). However, modern planktonic foraminifera at least do not compete for resources (Rillo et al., 2019). Another option is the presence of an unknown selection pressure acting upon these discrete populations, with a likely candidate being global temperature changes, where biserial forms are more adapted to a cooling water column than *Pseudohastigerina*. Indeed, planktonic foraminifera show relative thermal niche conservatism over million-year timescales (Waterson et al., 2017; Antell et al., 2021; Strack et al., 2022; Dowsett et al., 2023), and the declining abundance alongside dwarfing (Cordey et al., 1970; Nocchi et al., 1986; Wade and Pearson, 2008; Wade and Olsson, 2009) of pseudohastigerinids across the EOT may pinpoint temperature as the primary driver for the extinction of this genus.

Alongside the rise in upwelling/high-productivity/low-oxygen indicator taxa, high abundances of the small, low-trochospire ecogroup 1 form *A. collactea* are also observed in ORG-2, with *A. collactea* increasing from 43 % to 81 % amongst all *Acarinina* from 5491–5479 mbdt during ORG-2 and comprising 23 % of the entire foraminiferal assemblage at 5479 mbdt (Fig. 5). This dominance is similar to patterns observed across the Paleocene–Eocene Thermal Maximum (PETM; ∼ 56 Ma; Aze, 2022) of the southern and northern Tethyan margins, within which blooms of low-trochospiral acarininids have been associated with increased productivity (Oberhänsli and Beniamovskii, 2000; Guasti and Speijer, 2007). The high and persistent dominance of *A. collactea* in ORG-2 at Algodoal during the middle Eocene may therefore support other observations of pronounced upwelling along the western Atlantic margin at this time (Bice et al., 2000; Huber and Sloan, 2000; Wade et al., 2000, 2001; Sloan and Huber, 2001a, b; Witkowski et al., 2020, 2021). However, more localized changes may also have been at play, where peak mean/median grain sizes recorded on Ceara Rise to the NE (Fig. 2; Dobson et al., 2001) and increased fluxes of biogenic silica and barium on Demerara Rise to the NW (Renaudie et al., 2010) suggest increased terrigenous input may also be attributable to ORG-2. Our records of increased sedimentation rates within Algodoal during ORG-2 lend support to this hypothesis (Fig. 8). Disentangling the regional extent and contributing factors of these western Atlantic upwelling events warrants further study.

## 5 Conclusions

The planktonic foraminiferal faunas of the Algodoal Well are highly diverse, are typical of tropical early Paleogene environments, and provide reasonable age control within the Foz do Amazonas Basin, with Cenozoic (sub)tropical planktonic foraminiferal biozones E9, E10, and E14 identifiable. Preservation of planktonic foraminiferal shells varied throughout the section, but samples were generally well preserved and borderline "glassy", with the best-preserved specimens in the early Oligocene. However, significant calcite infill and overgrowth of shells throughout the study interval hinder the use of Algodoal as a low-latitude site of exceptional preservation for geochemical studies.

Relative abundance of planktonic foraminifera demonstrated dramatic long-term changes in assemblage character and composition associated with the gradual transition from the Eocene "greenhouse" to the Oligocene "icehouse" world. Significant changes in the thermal and trophic profile of the ocean led to the gradual loss in abundance and diversity of symbiont-bearing surface mixed-layer dwellers and increase amongst sub-thermocline dwellers at Algodoal, characteristic of global patterns. Superimposed on this long-term pattern, the presence of taxa indicative of upwelling/high-productivity surface waters, within two distinct organic-rich intervals in the middle Eocene and early Oligocene, were likely associated with regional upwelling and global palaeoceanographic changes. The identification of these macroevolutionary changes highlight the utility of functional group analyses for interpreting global macroevolutionary change on both the regional and global stage.

**Data availability.** Planktonic foraminiferal assemblage slides are to be accessioned into the Lapworth Museum of Geology, University of Birmingham. All other raw planktonic foraminiferal data are included in the Supplement.

**Supplement.** The supplement related to this article is available online at https://doi.org/10.5194/jm-44-601-2025-supplement.

**Author contributions.** Conceptualization: KME. Data curation: AW, KME, CH. Investigation: AW. Methodology: KME, AW, BW. Sample collection: CH. Taxonomy: AW, KME, BW. Writing: AW, KME, BW, CH, TDJ.

**Competing interests.** The contact author has declared that none of the authors has any competing interests.



**Acknowledgements.** We thank the Brazilian Oil and Gas Agency (ANP) for allowing us to study and publish on selected 1-BP-3 APS well samples and data (Well 2, following Figueiredo et al., 2009; Hoorn et al., 2017) and Petrobras for facilitating sample access and the technical discussions with their staff. Bridget S. Wade was supported by the UK Natural Environment Research Council (NERC) grant NE/V018361/1. Kirsty M. Edgar and Tom Dunkley Jones were supported by NERC grant NE/P013112/1. We thank Helena Hornsby for processing 10 samples utilized in this study, and we thank Nikol Staikidou and Paul Minton for conducting Z-stack light microscope imaging at UCL used in Plate 5. Finally, we would like to thank Helen Coxall and an anonymous reviewer for their time and productive comments.

**Financial support.** This research has been supported by the Natural Environment Research Council (grant nos. NE/V018361/1 and NE/P013112/1).

**Review statement.** This paper was edited by Sev Kender and reviewed by Helen Coxall and one anonymous referee.

## References

Agnini, C., Fornaciari, E., Giusberti, L., Grandesso, P., Lanci, L., Luciani, V., Muttoni, G., Pälike, H., Rio, D., Spofforth, D. J., and Stefani, C.: Integrated biomagnetostratigraphy of the Alano section (NE Italy): A proposal for defining the middle-late Eocene boundary, Bulletin, 123, 841–872, https://doi.org/10.1130/B30158.1, 2011.

Agnini, C., Fornaciari, E., Raffi, I., Catanzariti, R., Pälike, H., Backman, J., and Rio, D.: Biozonation and biochronology of Paleogene calcareous nannofossils from low and middle latitudes, Newslett. Stratigr., 47, 131–181, 2014.

Aljahdali, M. H., Elhag, M., Mufrreh, Y., Memesh, A., Alsoubhi, S., and Zalmout, I. S.: Upper Eocene calcareous nannofossil biostratigraphy: a new preliminary priabonian record from northern Saudi Arabia, Applied Ecology and Environmental Research, 18, https://doi.org/10.15666/aeer/1804_56075625, 2020.

Al-Sabouni, N., Kucera, M., and Schmidt, D. N.: Vertical niche separation control of diversity and size disparity in planktonic foraminifera, Mar. Micropaleontol., 63, 75–90, 2007.

Anagnostou, E., John, E. H., Edgar, K. M., Foster, G. L., Ridgwell, A., Inglis, G. N., Pancost, R. D., Lunt, D. J., and Pearson, P. N.: Changing atmospheric CO2 concentration was the primary driver of early Cenozoic climate, Nature, 533, 380–384, https://doi.org/10.1038/nature17423, 2016.

Antell, G. T., Fenton, I. S., Valdes, P. J., and Saupe, E. E.: Thermal niches of planktonic foraminifera are static throughout glacial–interglacial climate change, P. Natl. Acad. Sci. USA, 118, e2017105118, https://doi.org/10.1073/pnas.2017105118, 2021.

Anthonissen, D. E. and Ogg, J. G.: Cenozoic and Cretaceous biochronology of planktonic foraminifera and calcareous nannofossils, The geologic time scale, Elsevier, https://doi.org/10.1016/B978-0-444-59425-9.15003-6, 1083–1127, 2012.

Antoine, P. O., Yans, J., Castillo, A. A., Stutz, N., Abello, M. A., Adnet, S., Custódio, M. A., Benites-Palomino, A., Billet, G., Boivin, M., and Herrera, F.: Biotic community and landscape changes around the Eocene–Oligocene transition at Shapaja, Peruvian Amazonia: Regional or global drivers?, Global Planet. Change, 202, 103512, https://doi.org/10.1016/j.gloplacha.2021.103512, 2021.

Arimoto, J., Nishi, H., Kuroyanagi, A., Takashima, R., Matsui, H., and Ikehara, M.: Changes in upper ocean hydrography and productivity across the Middle Eocene Climatic Optimum: Local insights and global implications from the Northwest Atlantic, Global Planet. Change, 193, 103258, https://doi.org/10.1016/j.gloplacha.2020.103258, 2020.

Aze, T.: Unraveling ecological signals from a global warming event of the past, P. Natl. Acad. Sci. USA, 119, e2201495119, https://doi.org/10.1073/pnas.2201495119, 2022.

Aze, T., Ezard, T. H. G., Purvis, A., Coxall, H. K., Stuart, D. R. M., Wade, B. S., and Pearson, P. N.: A phylogeny of Cenozoic macroperforate planktonic foraminifera from fossil data, Biol. Rev., 86, 900–927, 2011.

Barrera, E. and Huber, B. T.: Paleogene and early Neogene oceanography of the southern Indian Ocean: Leg 119 foraminifer stable isotope results, Proc. Ocean Drill. Program, 119, 693–717, 1991.

Bayona, G., Cortés, M., Jaramillo, C., Ojeda, G., Aristizabal, J. J., and Reyes-Harker, A.: An integrated analysis of an orogen–sedimentary basin pair: Latest Cretaceous–Cenozoic evolution of the linked Eastern Cordillera orogen and the Llanos foreland basin of Colombia, Geol. Soc. Am. Bull., 120, 1171–1197, 2008.

Beckman, J. P.: The foraminifera and some associated microfossils of Sites 135 to 144, Initial Reports of the Deep Sea Drilling Project, Lisbon, Portugal to San Juan, Puerto Rico, Initial Reports of the Deep Sea Drilling Project, Vol. 14,Texas A&M University, Ocean Drilling Program, College Station, TX, USA, 389–420, https://doi.org/10.2973/dsdp.proc.14.113.1972, 1972.

Berggren, W. A.: Neogene planktonic foraminifer magnetobiostratigraphy of the southern Kerguelen Plateau (Sites 747, 748, and 751), in: Proceedings of the Ocean Drilling Program, Ocean Drilling Program, https://doi.org/10.2973.odp.proc.sr.120.153.1992, 1992.

Berggren, W. A. and Pearson, P. N.: A revised tropical and subtropical Paleogene planktonic foraminiferal zonation, J. Foraminifer. Res., 35, 279–298, 2005.

Berggren, W. A., Kent, D. V., and Flynn, J. J.: Jurassic to Paleogene: Part 2 Paleogene geochronology and chronostratigraphy, Geol. Soc. Lond. Memoirs, 10, 141–195, 1985.

Berggren, W. A., Pearson, P. N., Huber, B. T., and Wade, B. S.: Taxonomy, biostratigraphy, and phylogeny of Eocene Acarinina, in: Atlas of Eocene Planktonic Foraminifera, edited by: Pearson, P. N., Olsson, R. K., Huber, B. T., Hemleben, C., and Berggren, W. A., Cushman Foundation Special Publication 41, Cushman Foundation, 257–326, ISBN 9781970168365, 2006.

Bice, K. I., Sloan, L. C., and Barron, F. J.: Comparison of early Eocene isotopic paleotemperatures and the three-dimensional OGCM temperature field: the potential for use of model-derived surface water $\delta^{18}O$, in: Warm Climates in Earth History, edited by: Huber, B. T., MacLeod, K. G., and Wing, S. L., Cambridge University Press, Cambridge, 79–131, https://doi.org/10.1017/CBO9780511564512, 2000.

Blow, W. H.: The cainozoic globigerinida (Vol. 3), Leiden: Brill, ISBN 9789004059351, ISBN 9004059350, 1979.

Boersma, A. and Premoli Silva, I.: Terminal Eocene events: planktonic Foraminifera and isotopic evidence, in: Developments in Palaeontology and Stratigraphy, Vol. 9, Elsevier, 213–223, https://doi.org/10.1016/S0920-5446(08)70124-9, 1986.

Boersma, A. and Premoli Silva, I.: Atlantic Paleogene biserial heterohelicid foraminifera and oxygen minima, Paleoceanography, 4, 271–286, 1989.

Boersma, A. and Premoli Silva, I.: Distribution of Paleogene planktonic foraminifera – analogies with the Recent?, Palaeoceanogr. Palaeocl. Palaeoecol., 83, 29–48, 1991.

Boersma, A. and Shackleton, N. J.: Oxygen and carbon isotope record through the Oligocene, Site 366, Equatorial Atlantic, Initial Reports of the Deep Sea Drilling Project 41, 957–962, https://doi.org/10.2973/dsdp.proc.41.136.1978, 1977.

Boersma, A., Premoli Silva, I., and Shackleton, N. J.: Atlantic Eocene planktonic foraminiferal paleohydrographic indicators and stable isotope paleoceanography, Paleoceanography, 2, 287–331, 1987.

Bohaty, S. M., Zachos, J. C., Florindo, F., and Delaney, M. L.: Coupled greenhouse warming and deep-sea acidification of the Middle Eocene, Paleoceanography, 24, PA2207, https://doi.org/10.1029/2008PA001676, 2009.

Borrelli, C., Cramer, B. S., and Katz, M. E.: Bipolar Atlantic deep-water circulation in the middle-late Eocene: Effects of Southern Ocean gateway openings, Paleoceanography, 29, 308–327, 2014.

Boscolo-Galazzo, F., Crichton, K. A., Ridgwell, A., Mawbey, E. M., Wade, B. S., and Pearson, P. N.: Temperature controls carbon cycling and biological evolution in the ocean twilight zone, Science, 371, 1148–1152, https://doi.org/10.1126/science.abb6643, 2021.

Boscolo-Galazzo, F., Jones, A., Dunkley Jones, T., Crichton, K. A., Wade, B. S., and Pearson, P. N.: Late Neogene evolution of modern deep-dwelling plankton, Biogeosciences, 19, 743–762, https://doi.org/10.5194/bg-19-743-2022, 2022.

Bown, P., Coe, A., Cope, J., Edgar, K., Harper, D., Marshall, J., Wakefield, M., Pearson, P. N., and Zalasiewicz, J.: Biostratigraphy – using fossils to date and correlate rock, in: Deciphering Earth's History: the Practice of Stratigraphy, edited by: Coe, A. L., Geological Society of London, ISBN 9781786205742, https://doi.org/10.1144/GIP1-2022-42, 2022.

Bown, P. R., Dunkley Jones, T., Lees, J. A., Randell, R. D., Mizzi, J. A., Pearson, P. N., Coxall, H. K., Young, J. R., Nicholas, C. J., Karega, A., Singano, J., and Wade, B. S.: A Paleogene calcareous microfossil Konservat-Lagerstätte from the Kilwa Group of coastal Tanzania, Geol. Soc. Am. Bull., 120, 3–12, 2008.

Boyle, P. R., Romans, B. W., Tucholke, B. E., Norris, R. D., Swift, S. A., and Sexton, P. F.: Cenozoic North Atlantic deep circulation history recorded in contourite drifts, offshore Newfoundland, Canada, Mar. Geol., 385, 185–203, 2017.

Brandão, J. A. S. and Feijó, F. J.: Bacia da Foz do Amazonas, Boletim de Geosciências da Petrobrás, 8, 91–99, 1994.

Broecker, W. S. and Clark, E.: $CaCO_3$ size index paleocarbonate ion proxy?, Paleoceanography, 14, 596–604, 1999.

Brombacher, A., Wilson, P. A., Bailey, I., and Ezard, T. H.: The dynamics of diachronous extinction associated with climatic deterioration near the Neogene/Quaternary boundary, Paleoceanography and Paleoclimatology, 36, e2020PA004205, 2021.

Bryant, R., Leckie, R. M., Bralower, T. J., Jones, M. M., and Sageman, B. B.: Microfossil and geochemical records reveal high-productivity paleoenvironments in the Cretaceous Western Interior Seaway during Oceanic Anoxic Event 2, Palaeogeogr. Palaeocl. Palaeoecol., 584, 110679, https://doi.org/10.1016/j.palaeo.2021.110679, 2021.

Castro, J. C., Miura, K., and Braga, J. A. E.: Stratigraphic and structural framework of the Foz do Amazonas, in: 10th Annual Offshore Technology Conference, 1843–1847, https://doi.org/10.4043/3265-MS, 1978.

Coccioni, R., Monaco, P., Monechi, S., Nocchi, M., and Parisi, G.: Biostratigraphy of the Eocene–Oligocene boundary at Massignano (Ancona, Italy), International Subcommission on Paleogene Stratigraphy, 50–80, 1988.

Cordey, W. G., Berggren, W. A., and Olsson, R. K.: Phylogenetic trends in the planktonic foraminiferal genus Pseudohastigerina Banner and Blow, 1959, Micropaleontology, 16, 235–242, 1970.

Coxall, H. K.: Hantkeninid planktonic foraminifera and Eocene palaeoceanographic change, Doctoral dissertation, University of Bristol, 2000.

Coxall, H. K. and Pearson, P. N.: Taxonomy, biostratigraphy, and phylogeny of the Hantkeninidae (Clavigerinella, Hantkenina, and Cribrohantkenina), edited by: Pearson, P. N., Olsson, R. K., Huber, B. T., Hemleben, C., and Berggren, W. A., Atlas of Eocene Planktonic Foraminifera : Cushman Foundation Special Publication, 41, 216–256, ISBN 9781970168365, 2006.

Coxall, H. K. and Pearson, P. N.: The Eocene-Oligocene transition, Deep Time Perspect. Clim. Chang. Marrying Signal From Comput. Model. Biol. Proxies, The Micropalaeontological Society, Special Publications, The Geological Society, London, UK, 351–387, https://doi.org/10.1144/TMS002.16, 2007.

Coxall, H. K., Pearson, P. N., Shackleton, N. J., and Hall, M. A.: Hantkeninid depth adaptation: an evolving life strategy in a changing ocean, Geology, 28, 87–90, 2000.

Coxall, H. K., Huber, B. T., and Pearson, P. N.: Origin and morphology of the Eocene planktonic foraminifer Hantkenina, J. Foraminifer. Res., 33, 237–261, 2003.

Coxall, H. K. and Spezzaferri, S.: Taxonomy, biostratigraphy, and phylogeny of Oligocene Catapsydrax, Globorotaloides, and Protentelloides, in: Atlas of Oligocene Planktonic Foraminifera, Cushman Foundation of Foraminiferal Research, Special Publi55 cation 46, edited by: Wade, B. S., Olsson, R. K., Pearson, P. N., Huber, B. T., and Berggren, W. A., Cushman Foundation, ISBN 9781970168419, 2018.

Coxall, H. K., Huck, C. E., Huber, M., Lear, C. H., Legarda-Lisarri, A., O'regan, M., Sliwinska, K. K., Van De Flierdt, T., De Boer, A. M., Zachos, J. C., and Backman, J.: Export of nutrient rich Northern Component Water preceded early Oligocene Antarctic glaciation, Nat. Geosci., 11, 190–196, 2018.

Coxall, H. K., Jones, T. D., Jones, A. P., Lunt, P., MacMillan, I., Marliyani, G. I., Nicholas, C. J., O'Halloran, A., Piga, E., Sanyoto, P., Rahardjo, W., and Pearson, P. N.: The Eocene–Oligocene transition in Nanggulan, Java: lithostratigraphy, biostratigraphy and foraminiferal stable isotopes, J. Geol. Soc., 178, jgs2021-2006, https://doi.org/10.1144/jgs2021-006, 2021.

Cramer, B. S., Miller, K. G., Barrett, P. J., and Wright, J. D.: Late Cretaceous–Neogene trends in deep ocean temperature and continental ice volume: Reconciling records of benthic foraminiferal geochemistry ($\delta^{18}$O and Mg/Ca) with sea level history, Journal of Geophysical Research: Oceans, 116, https://doi.org/10.1029/2011JC007255, 2011.

Cramer, B. S., Toggweiler, J. R., Wright, J. D., Katz, M. E., and Miller, K. G.: Ocean overturning since the Late Cretaceous: Inferences from a new benthic foraminiferal isotope composition, Paleoceanography, 24, PA4216, https://doi.org/10.1029/2008PA001683, 2009.

Defant, A.: Physical Oceanography, vol. 2, Pergamon, New York, 1961.

D'Hondt, S., Zachos, J. C., and Schultz, G.: Stable isotopic signals and photosymbiosis in late Paleocene planktic foraminifera. Paleobiology, 20, 391–406, https://doi.org/10.1017/S0094837300012847, 1994.

Dobson, D. M., Dickens, G. R., and Rea, D. K.: Terrigenous sediment on Ceara Rise: a Cenozoic record of South American orogeny and erosion, Palaeogeogr. Palaeocl., Palaeoecol., 165, 215–229, 2001.

D'Onofrio, R., Luciani, V., Dickens, G. R., Wade, B. S., and Kirtland-Turner, S.: Demise of the planktic foraminifer genus Morozovella during the early Eocene climatic optimum: New records from ODP site 1258 (Demerara Rise, Western Equatorial Atlantic) and site 1263 (Walvis Ridge, South Atlantic), Geosciences, 10, 88, https://doi.org/10.3390/geosciences10030088, 2020.

Douglas, R. G.: Planktonic foraminiferal biostratigraphy in the Central North Pacific Ocean, Initial Reports of the Deep Sea Drilling Project, Vol. 17, Texas A&M University, Ocean Drilling Program, College Station, TX, USA, 673–694, https://doi.org/10.2973/dsdp.proc.17.122.1973, 1973.

Douglas, R. G. and Savin, S. M.: Oxygen isotopic evidence for the depth stratification of Tertiary and Cretaceous planktic foraminifera, Marine Micropaleontology, 3, 175–196, https://doi.org/10.1016/0377-8398(78)90004-X, 1978.

Dowsett, H., Robinson, M., Foley, K., Herbert, T., Hunter, S., Andersson, C., and Spivey, W.: The Relative Stability of Planktic Foraminifer Thermal Preferences over the Past 3 Million Years, Geosciences, 13, 71, https://doi.org/10.3390/geosciences13030071, 2023.

Duarte, D., Erba, E., Bottini, C., Wagner, T., Aduomahor, B., Jones, T. D. and Nicholson, U.: Early Cretaceous deep-water bedforms west of the Guinea Plateau revise the opening history of the Equatorial Atlantic Gateway. Global Planet. Change, 249, 104777, https://doi.org/10.1016/j.gloplacha.2025.104777, 2025.

Edgar, K. M., Wilson, P. A., Sexton, P. F., Gibbs, S. J., Roberts, A. P., and Norris, R. D.: New biostratigraphic, magnetostratigraphic and isotopic insights into the Middle Eocene Climatic Optimum in low latitudes, Palaeogeogr. Palaeocl. Palaeoecol., 297, 670–682, 2010.

Edgar, K. M., Bohaty, S. M., Gibbs, S. J., Sexton, P. F., Norris, R. D., and Wilson, P. A.: Symbiont 'bleaching' in planktic foraminifera during the Middle Eocene Climatic Optimum, Geology, 41, 15–18, 2013.

Edgar, K. M., Anagnostou, E., Pearson, P. N., and Foster, G. L.: Assessing the impact of diagenesis on $\delta^{11}$B, $\delta^{13}$C, $\delta^{18}$O, Sr/Ca and B/Ca values in fossil planktic foraminiferal calcite, Geochim. Cosmochim. Ac., 166, 189–209, 2015.

Edgar, K. M., Hull, P. M., and Ezard, T. H.: Evolutionary history biases inferences of ecology and environment from $\delta^{13}$C but not $\delta^{18}$O values, Nat. Commun., 8, 1106, https://doi.org/10.1038/s41467-017-01154-7, 2017.

Edgar, K. M., Bohaty, S. M., Coxall, H. K., Bown, P. R., Batenburg, S. J., Lear, C. H., and Pearson, P. N.: New composite bio- and isotope stratigraphies spanning the Middle Eocene Climatic Optimum at tropical ODP Site 865 in the Pacific Ocean, J. Micropalaeontol., 39, 117–138, 2020.

Egan, K. E., Rickaby, R. E., Hendry, K. R., and Halliday, A. N.: Opening the gateways for diatoms primes Earth for Antarctic glaciation, Earth Planet. Sc. Lett., 375, 34–43, 2013.

Erhardt, A. M., Pälike, H., and Paytan, A.: High-resolution record of export production in the eastern equatorial Pacific across the Eocene–Oligocene transition and relationships to global climatic records, Paleoceanography, 28, 130–142, 2013.

Expedition 320/321 Scientists: Site U1332, in: Proc. IODP, 320/321, edited by: Pälike, H., Lyle, M., Nishi, H., Raffi, I., Gamage, K., Klaus, A., and the Expedition 320/321 Scientists, Integrated Ocean Drilling Program Management International, Inc., Tokyo, https://doi.org/10.2204/iodp.proc.320321.104.2010, 2010a.

Expedition 320/321 Scientists: Site U1333, in: Proc. IODP, 320/321, edited by: Pälike, H., Lyle, M., Nishi, H., Raffi, I., Gamage, K., Klaus, A., and the Expedition 320/321 Scientists, Integrated Ocean Drilling Program Management International, Inc., Tokyo, https://doi.org/10.2204/iodp.proc.320321.105.2010, 2010b.

Expedition 320/321 Scientists: Site U1334, in: Proc. IODP, 320/321, edited by: Pälike, H., Lyle, M., Nishi, H., Raffi, I., Gamage, K., Klaus, A., and the Expedition 320/321 Scientists, Integrated Ocean Drilling Program Management International, Inc., Tokyo, https://doi.org/10.2204/iodp.proc.320321.106.2010, 2010c.

Ezard, T. H. G., Aze, T., Pearson, P. N., and Purvis, A.: Interplay between changing climate and species' ecology drives macroevolutionary dynamics, Science, 332, 349–351, 2011.

Faith, D. P., Minchin, P. R., and Belbin, L.: Compositional dissimilarity as a robust measure of ecological distance, Vegetatio, 69, 57–68, 1987.

Fenton, I. S., Woodhouse, A., Aze, T., Lazarus, D., Renaudie, J., Dunhill, A. M., Young, J. R., and Saupe, E. E.: Triton, a new species-level database of Cenozoic planktonic foraminiferal occurrences. Sci. Data, 8, 160, https://doi.org/10.1038/s41597-021-00942-7, 2021.

Figueiredo, J. J. J. P., Hoorn, C., Van der Ven, P., and Soares, E.: Late Miocene onset of the Amazon River and the Amazon deep-sea fan: Evidence from the Foz do Amazonas Basin, Geology, 37, 619–622, 2009.

Filippi, G., Barrett, R., Schmidt, D. N., D'Onofrio, R., Westerhold, T., Brombin, V., and Luciani, V.: Impacts of the Early Eocene Climatic Optimum (EECO,∼ 53-49 Ma) on Planktic Foraminiferal Resilience, Paleoceanography and Paleoclimatology, 39, e2023PA004820, 2024.

Flannery-Sutherland, J. T., Raja, N. B., Kocsis, Á. T., and Kiessling, W.: Fossilbrush: An R package for automated detection and resolution of anomalies in palaeontological occurrence data, Methods in Ecology and Evolution, 13, 2404–2418, https://doi.org/10.1111/2041-210X.13966, 2022.

Fleisher, R. L.: Cenozoic planktonic foraminifera and biostratigraphy, Arabian Sea, Deep Sea Drilling Project, Leg 23A, in: Init. Repts. DSDP 23, edited by: Whitmarsh, R. B., US Govt. Printing Office, Washington, 1001–1072, https://doi.org/10.2973/dsdp.proc.23.139.1974, 1974.

Fluegeman, R. H.: Preliminary paleontological report on the foraminifera of the Mossy Grove core, Hinds County, Mississippi, Mississippi Geology, 17, 9–15, 1996.

Fluegeman, R. H., Grigsby, J. D., and Hurley, J. V.: Eocene-Oligocene greenhouse to icehouse transition on a subtropical clastic shelf, the Jackson-Vicksburg Groups of the eastern Gulf Coastal Plain of the United States, Spec. Pap. -Geol. Soc. Am., 452, 261–277, 2009.

Fofonoff, N. P.: Machine computations of mass transport in the North Pacific Ocean, Journal of the Fisheries Board of Canada, 19, 1121–1141, 1962.

Fornaciari, E., Agnini, C., Catanzariti, R., Rio, D., Bolla, M. E., and Valvasoni, E.: Mid-latitude calcareous nannofossil biostratigraphy and biochronology across the middle to late Eocene transition, Stratigraphy, 7, 229–264, 2010.

Foster, G. L., Royer, D. L., and Lunt, D. J.: Future climate forcing potentially without precedent in the last 420 million years, Nature communications, 8, 14845, 2017.

Fraass, A. J., Kelly, D. C., and Peters, S. E.: Macroevolutionary history of the planktic foraminifera, Annual Review of Earth and Planetary Sciences, 43, 139–166, https://doi.org/10.1146/annurev-earth-060614-105059, 2015.

Gaskell, D. E., Huber, M., O'Brien, C. L., Inglis, G. N., Acosta, R. P., Poulsen, C. J., and Hull, P. M.: The latitudinal temperature gradient and its climate dependence as inferred from foraminiferal $\delta^{18}$O over the past 95 million years, Proceedings of the National Academy of Sciences, 119, e2111332119, 2022.

Gómez, E., Jordan, T. E., Allmendinger, R. W., Hegarty, K., Kelley, S., and Heizler, M.: Controls on architecture of the late Cretaceous to Cenozoic southern middle Magdalena valley basin, Colombia, Geol. Soc. Am. Bull., 115, 131–147, 2003.

Gradstein, F., Ogg, J. G., Schmitz, M. D., and Ogg, G. M. (Eds.): The geologic time scale 2012, Elsevier, ISBN 978-0-444-59425-9, 2012.

Griffith, E. M., Paytan, A., Eisenhauer, A., Bullen, T. D., and Thomas, E.: Seawater calcium isotope ratios across the Eocene–Oligocene transition, Geology, 39, 683–686, 2011.

Guasti, E. and Speijer, R. P.: The Paleocene-Eocene Thermal Maximum in Egypt and Jordan: An overview of the planktic foraminiferal record, in: Large ecosystem perturbations: Causes and consequences, Geological Society of America Special Paper 424, edited by: Monechi, S., Coccioni, R., and Rampino, M., Geological Society of America, 53–67, https://doi.org/10.1130/2007.2424(03), 2007.

Hallock, P.: Why are large Foraminifera large?, Paleobiology, 11, 195–208, 1985.

Hancock, H. J. L. and Dickens, G. R.: Carbonate dissolution episodes in Paleocene and Eocene sediment, Shatsky Rise, west-central Pacific, in: Proceedings of the Ocean Drilling Program, Scientific Results 198, edited by: Bralower, T. J., Premoli Silva, I., and Malone, M. J., 1–24, https://doi.org/10.2973/odp.proc.sr.198.116.2005, 2005.

Hayward, B. W., Grenfell, H. R., Reid, C. M., and Hayward, K. A.: Recent New Zealand shallow-water benthic foraminifera: taxonomy, ecologic distribution, biogeography, and use in paleoenvironmental assessment, New Zealand Geological Survey Bulletin, 75, 1999.

Heine, C., Zoethout, J. and Müller, R. D.: Kinematics of the South Atlantic rift, Solid Earth, 4, 215–253, https://doi.org/10.5194/se-4-215-2013, 2013.

Hohbein, M. W., Sexton, P. F., and Cartwright, J. A.: Onset of North Atlantic Deep Water production coincident with inception of the Cenozoic global cooling trend, Geology, 40, 255–258, 2012.

Hoorn, C. and Wesselingh, F.: Amazonia: Landscape and species evolution, Blackwell Publishing, Chichester, 210 pp., https://doi.org/10.1002/9781444306408, 2010.

Hoorn, C., Bogotá-A, G. R., Romero-Baez, M., Lammertsma, E. I., Flantua, S. G., Dantas, E. L., Dino, R., do Carmo, D. A., and Chemale Jr., F.: The Amazon at sea: Onset and stages of the Amazon River from a marine record, with special reference to Neogene plant turnover in the drainage basin, Global Planet. Change, 153, 51–65, 2017.

Houben, A. J., Bijl, P. K., Sluijs, A., Schouten, S., and Brinkhuis, H.: Late Eocene Southern Ocean cooling and invigoration of circulation preconditioned Antarctica for full-scale glaciation, Geochem. Geophy. Geosy., 20, 2214–2234, 2019.

Huber, B. T. and Sloan, L. C.: Modelling the Paleogene: Part II. Paleogene wind-driven circulation changes predicted from climatic modelling studies, Geologiska Foreningens i Stokholm Forhandlingar, 122, 80–81, 2000.

Huber, B. T., Olsson, R. K., and Pearson, P. N.: Taxonomy, biostratigraphy, and phylogeny of Eocene microperforate planktonic foraminifera (Jenkinsina, Cassigerinelloita, Chiloguembelina, Streptochilus, Zeauvigerina, Tenuitella, and Cassigerinella) and Problematica (Dipsidripella), in: Atlas of Eocene Planktonic Foraminifera, Cushman Foundation Special Publication 41, edited by: Pearson, P. N., Olsson, R. K., Huber, B. T., Hemleben, C., and Berggren, W. A., Cushman Foundation, 461–508, ISBN 9781970168365, 2006.

Huber, B. T., Petrizzo, M. R., Young, J. R., Falzoni, F., Gilardoni, S. E., Bown, P. R. and Wade, B. S.: Pforams@ microtax, Micropaleontology, 62(6), pp. 429–438, 2016.

Hutchinson, D. K., Coxall, H. K., O'Regan, M., Nilsson, J., Caballero, R., and de Boer, A. M.: Arctic closure as a trigger for Atlantic overturning at the Eocene–Oligocene Transition, Nat. Commun., 10, 3797, https://doi.org/10.1038/s41467-019-11828-z, 2019.

Hutchinson, D. K., Coxall, H. K., Lunt, D. J., Steinthorsdottir, M., de Boer, A. M., Baatsen, M., von der Heydt, A., Huber, M.,

Kennedy-Asser, A. T., Kunzmann, L., Ladant, J.-B., Lear, C. H., Moraweck, K., Pearson, P. N., Piga, E., Pound, M. J., Salzmann, U., Scher, H. D., Sijp, W. P., Śliwińska, K. K., Wilson, P. A., and Zhang, Z.: The Eocene–Oligocene transition: a review of marine and terrestrial proxy data, models and model–data comparisons, Clim. Past, 17, 269–315, https://doi.org/10.5194/cp-17-269-2021, 2021.

Hyland, E. G. and Sheldon, N. D.: Coupled CO2-climate response during the early Eocene climatic optimum. Palaeogeography, Palaeoclimatology, Palaeoecology, 369, 125–135, https://doi.org/10.1016/j.palaeo.2012.10.011, 2013.

Inglis, G. N., Farnsworth, A., Lunt, D., Foster, G. L., Hollis, C. J., Pagani, M., Jardine, P. E., Pearson, P. N., Markwick, P., Galsworthy, A. M., and Raynham, L.: Descent toward the Icehouse: Eocene sea surface cooling inferred from GDGT distributions, Paleoceanography, 30, 1000–1020, 2015.

Inglis, G. N., Bragg, F., Burls, N. J., Cramwinckel, M. J., Evans, D., Foster, G. L., Huber, M., Lunt, D. J., Siler, N., Steinig, S., Tierney, J. E., Wilkinson, R., Anagnostou, E., de Boer, A. M., Dunkley Jones, T., Edgar, K. M., Hollis, C. J., Hutchinson, D. K., and Pancost, R. D.: Global mean surface temperature and climate sensitivity of the early Eocene Climatic Optimum (EECO), Paleocene–Eocene Thermal Maximum (PETM), and latest Paleocene, Clim. Past, 16, 1953–1968, https://doi.org/10.5194/cp-16-1953-2020, 2020.

John, E. H., Pearson, P. N., Coxall, H. K., Birch, H., Wade, B. S., and Foster, G. L.: Warm ocean processes and carbon cycling in the Eocene. Philosophical Transactions of the Royal Society A: Mathematical, Physical and Engineering Sciences, 371, 20130099, https://doi.org/10.1098/rsta.2013.0099, 2013.

Jones, A. P. and Dunkley Jones, T.: Middle Eocene to early Oligocene calcareous nannofossils from the Nanggulan Formation, Java, Indonesia, J. Nannoplankt. Res., 38, 57–79, 2020.

Jones, A. P., Dunkley Jones, T., Coxall, H., Pearson, P. N., Nala, D., and Hoggett, M.: Low-latitude calcareous nannofossil response in the Indo-Pacific warm pool across the Eocene–Oligocene transition of Java, Indonesia, Paleoceanogr. Paleoclimatol., 34, 1833–1847, 2019.

Jones, M. M., Sageman, B. B., Selby, D., Jacobson, A. D., Batenburg, S. J., Riquier, L., MacLeod, K. G., Huber, B. T., Bogus, K. A., Tejada, M. L. G., and Kuroda, J.: Abrupt episode of mid-Cretaceous ocean acidification triggered by massive volcanism, Nat. Geosci., 16, 169–174, 2023.

Katz, M. E., Cramer, B. S., Toggweiler, J. R., Esmay, G., Liu, C., Miller, K. G., Rosenthal, Y., Wade, B. S., and Wright, J. D.: Impact of Antarctic Circumpolar Current development on late Paleogene ocean structure, Science, 332, 1076–1079, 2011.

Kearns, L. E., Bohaty, S. M., Edgar, K. M., Nogué, S., and Ezard, T. H.: Searching for function: reconstructing adaptive niche changes using geochemical and morphological data in planktonic foraminifera, Front. Ecol. Evol., 9, 679722, https://doi.org/10.3389/fevo.2021.679722, 2021.

Kearns, L. E., Bohaty, S. M., Edgar, K. M., and Ezard, T. H. G.: Small but mighty: how overlooked small species maintain community structure through middle Eocene climate change, Paleobiology, 49, 77–98, 2023.

Keller, G.: Biochronology and paleoclimatic implications of Middle Eocene to Oligocene planktonic foraminiferal faunas, Mar. Micropaleontol., 7, 463–486, 1983.

Keller, G., MacLeod, N., and Barrera, E.: Eocene–Oligocene faunal turnover in planktic foraminifer, and Antarctic glaciation, in: Eocene–Oligocene climatic and biotic evolution, edited by: Prothero, D. R. and Berggren, W. A., Princeton University Press, Princeton, 218–244, ISBN 978-1-4008-6292-4, 1992.

Kelly, D. C.: Response of Antarctic (ODP Site 690) planktonic foraminifera to the Paleocene–Eocene thermal maximum: faunal evidence for ocean/climate change, Paleoceanography, 17, 1–13, 2002.

Kennett, J. P., Houtz, R. E., Andrews, P. B., Edwards, A. R., Gostin, V. A., Hajós, M., Hampton, M., Jenkins, D. G., Margolis, S. V., Ovenshine, A. T., and Perch-Nielsen, K.: Cenozoic paleoceanography in the southwest Pacific Ocean, Antarctic glaciation, and the development of the Circum-Antarctic Current, Initial reports of the deep sea drilling project, U.S. Government Printing Office, Washington, D.C., 29, 1155–1169, https://doi.org/10.2973/dsdp.proc.29.144.1975, 1975.

King, D. J. and Wade, B. S.: The extinction of Chiloguembelina cubensis in the Pacific Ocean: implications for defining the base of the Chattian (upper Oligocene), Newslett. Stratigr., 50, 311–339, 2017.

Krashininnikov, V. A. A.: Cenozoic Foraminifera. In. Initial reports of the Deep Sea Drilling Project, covering Leg 6 of the cruises of the drilling vessel "Glomar Challenger", Honolulu, Hawaii to Apra, Guam, June–August, 1969, in: Initial Reports of the Deep Sea Drilling Project, Vol. 6, edited by: Fischer, A. G., Heezen, B. C., Boyce, R. E., Bukry, J. D., Douglas, R. G., Garrison, R. E., Kling, S. A., Krasheninnikov, V. A. A., Lisitzin, A. P., and Pimm., A. C., Texas A&M University, Ocean Drilling Program, College Station, TX, USA, 1055–1068, https://doi.org/:10.2973/dsdp.proc.6.133.1971, 1971.

Krause, A. J., Sluijs, A., Van der Ploeg, R., Lenton, T. M., and Pogge von Strandmann, P. A.: Enhanced clay formation key in sustaining the Middle Eocene Climatic Optimum, Nat. Geosci., 16, 730–738, 2023.

Lam, A. R., Crundwell, M. P., Leckie, R. M., Albanese, J., and Uzel, J. P.: Diachroneity rules the mid-latitudes: A test case using Late Neogene planktic foraminifera across the Western Pacific, Geosciences, 12, 190, https://doi.org/10.3390/geosciences12050190, 2022.

Lammertsma, E. I., Troelstra, S. R., Flores, J. A., Sangiorgi, F., Chemale Jr., F., do Carmo, D. A., and Hoorn, C.: Primary productivity in the western tropical Atlantic follows Neogene Amazon River evolution, Palaeogeogr. Palaeocl. Palaeoecol., 506, 12–21, 2018.

Lazarus, D., Weinkauf, M., and Diver, P.: Pacman profiling: a simple procedure to identify stratigraphic outliers in high-density deep-sea microfossil data, Paleobiology, 38, 144–161, https://doi.org//10.1666/10067.1, 2012.

Leckie, R. M.: A paleoceanographic model for the early evolutionary history of planktonic foraminifera. Palaeogeography, Palaeoclimatology, Palaeoecology, 73, 107–138, https://doi.org/10.1016/0031-0182(89)90048-5, 1989.

Leckie, M., Farnham, C., and Schmidt, M. G.: Oligocene planktonic foraminifer biostratigraphy of Hole 803D (Ontong Java Plateau) and Hole 628A (Little Bahama Bank), and comparison with the southern high latitudes, in: Proceedings of the Ocean Drilling Program, Scientific Results, edited by: Berger, W. H., Kroenke, L. W., Janecek, T. R., Backman, J., Bassinot,

F., Corfield, R. M., Delaney, M. L., Hagen, R., Jansen, E., Krissek, L. A., Lange, C., Leckie, R. M., Lind, I. L., Lyle, M. W., Mahoney, J. J., Marsters, J. C., Mayer, L., Mosher, D. C., Musgrave, R., Prentice, M. L., Resig, J. M., Schmidt, H., Stax, R., Storey, M., Takahashi, K., Takayama, T., Tarduno, J.A., Wilkens, R. H., Wu, G., and Maddox, E. M., Ocean Drilling Program College Station, Texas, USA, 130, 113–136, https://doi.org/10.2973/odp.proc.sr.130.012.1993, 1993.

Leckie, R. M., Yuretich, R. F., West, O. L., Finkelstein, D., and Schmidt, M.: Paleoceanography of the southwestern Western Interior Sea during the time of the Cenomanian-Turonian boundary (Late Cretaceous), edited by: Dean, W., and Arthur, M. A., Stratigraphy and Paleoenvironments of the Cretaceous Western Interior Seaway, SEPM Concepts in Sedimentology and Paleontology, vol. 6, 101–126, https://doi.org/10.2110/csp.98.06.0101, 1998.

Leckie, R. M., Wade, B. S., Pearson, P. N., Fraass, A. J., King, D. J., Olsson, R. K., Silva, I. P., Spezzaferri, S., and Berggren, W. A.: Taxonomy, biostratigraphy, and phylogeny of Oligocene and early Miocene Paragloborotalia and Parasubbotina, in: Atlas of Oligocene Planktonic Foraminifera, Cushman Foundation of Foraminiferal Research, Special Publication 46, edited by: Wade, B. S., Olsson, R. K., Pearson, P. N., Huber, B. T., and Berggren, W. A., Cushman Foundation, ISBN 9781970168419, 2018.

Liu, C., Browning, J. V., Miller, K. G., and Olsson, R. K.: Upper Cretaceous to Miocene planktonic foraminiferal biostratigraphy: Results of Leg 150X, the New Jersey Coastal Plain Drilling Project, in: Proceedings of the Ocean Drilling Program, Scientific Results, edited by: Miller, K. G. and Snyder, S. W., Ocean Drilling Program College Station, Texas, USA, 150X, 111-127, https://doi.org/10.2973/odp.proc.sr.150x.308.1997, 1997.

Liu, Z., Pagani, M., Zinniker, D., DeConto, R., Huber, M., Brinkhuis, H., Shah, S. R., Leckie, R. M., and Pearson, A.: Global cooling during the Eocene–Oligocene climate transition, Science, 323, 1187–1190, 2009.

Liow, L. H., Skaug, H. J., Ergon, T., and Schweder, T.: Global occurrence trajectories of microfossils: environmental volatility and the rise and fall of individual species, Paleobiology, 36, 224–252, https://doi.org/10.1666/08080.1, 2010.

Lowery, C. M., Bown, P. R., Fraass, A. J., and Hull, P. M.: Ecological response of plankton to environmental change: thresholds for extinction. Annual Review of Earth and Planetary Sciences, 48, 403–429, https://doi.org/10.1146/annurev-earth-081619-052818, 2020.

Luciani, V., Giusberti, L., Agnini, C., Fornaciari, E., Rio, D., Spofforth, D. J. A., and Pälike, H.: Ecological and evolutionary response of Tethyan planktonic foraminifera to the middle Eocene climatic optimum (MECO) from the Alano section (NE Italy), Palaeogeogr. Palaeocl. Palaeoecol., 292, 82–95, 2010.

Luciani, V., Dickens, G. R., Backman, J., Fornaciari, E., Giusberti, L., Agnini, C., and D'Onofrio, R.: Major perturbations in the global carbon cycle and photosymbiont-bearing planktic foraminifera during the early Eocene, Clim. Past, 12, 981–1007, https://doi.org/10.5194/cp-12-981-2016, 2016.

Luciani, V., D'Onofrio, R., Dickens, G. R., and Wade, B. S.: Planktic foraminiferal response to early Eocene carbon cycle perturbations in the southeast Atlantic Ocean (ODP Site 1263), Global Planet. Change, 158, 119–133, https://doi.org/10.1016/j.gloplacha.2017.09.007, 2017a.

Luciani, V., D'Onofrio, R., Dickens, G. R., and Wade, B. S.: Did Photosymbiont Bleaching Lead to the Demise of Planktic Foraminifer Morozovella at the Early Eocene Climatic Optimum?: Early Eocene Photosymbiont Bleaching, Paleoceanography, 32, 1115–1136, https://doi.org/10.1002/2017PA003138, 2017b.

Luciani, V., D'Onofrio, R., Dickens, G. R., and Wade, B. S.: Dextral to sinistral coiling switch in planktic foraminifer Morozovella during the Early Eocene Climatic Optimum, Global Planet. Change, 206, 103634, https://doi.org/10.1016/j.gloplacha.2021.103634, 2021.

Majewski, W.: Water-depth distribution of Miocene planktonic foraminifera from ODP Site 744, Southern Indian Ocean, The Journal of Foraminiferal Research, 33, 144–154, https://doi.org/10.2113/0330144, 2003.

McCave, I. N.: Chapter one deep-sea sediment deposits and properties controlled by currents, Dev. Mar. Geol., 1, 19–62, 2007.

McGowran, B.: Foraminifera, Initial Reports of the Deep Sea Drilling Project, https://doi.org/10.2973/dsdp.proc.22.128.1974, 1974.

McGowran, B.: Cenozoic environmental shifts and foraminiferal evolution. In Earth and life: Global biodiversity, extinction intervals and biogeographic perturbations through time, Dordrecht: Springer Netherlands, 937–965, https://doi.org/10.1007/978-90-481-3428-1_33, 2012.

McNown, J. S. and Malaika, J.: Effects of particle shape on settling velocity at low Reynolds numbers. Eos, Transactions American Geophysical Union, 31, 74–82, https://doi.org/10.1029/TR031i001p00074, 1950.

Mello, M. R., Mosmann, R., Silva, S. R. P., Maciel, R. R., and Miranda, F. P.: Foz do Amazonas area: The last frontier for elephant hydrocarbon accumulations in the South Atlantic realm, in: Petroleum provinces of the twenty-first century, edited by: Downey, M. W., Threet, J. C., and Morgan, W. A., AAPG Memoir, 74, 403–414, 2001.

Miller, K. G., Browning, J. V., Aubry, M. -P., Wade, B. S., Katz., M. E., Kulpecz, A. A., and Wright, J. D.: Eocene–Oligocene global climate and sea-level: St. Stephens Quarry, Alabama, Geol. Soc. Am. Bull., 120, 34–53, 2008.

Mohriak, W. U.: Bacias Sedimentares da Margem Continental Brasileria, in: Geologia, tectônica e recursos minerais do Brasil, edited by: Lizzi, L. A., Schobbenhaus, C., Vidotti, R. M., and Gon?alves, J. H., CPRM, Brasilia, 131 pp., 2003.

Moore Jr., T. C., Wade, B. S., Westerhold, T., Erhardt, A. M., Coxall, H. K., Baldauf, J., and Wagner, M.: Equatorial Pacific productivity changes near the Eocene–Oligocene boundary, Paleoceanography, 29, 825–844, 2014.

Mora, A., Baby, P., Roddaz, M., Parra, M., Brusset, S., Hermoza, W., and Espurt, N.: Tectonic history of the Andes and sub-Andean zones: implications for the development of the Amazon drainage basin. Amazonia, landscape and species evolution: a look into the past, Wiley-Blackwell, 38–60, https://doi.org/10.1002/9781444306408.ch4, 2010.

Müller, R. D., Seton, M., Zahirovic, S., Williams, S. E., Matthews, K. J., Wright, N. M., Shephard, G. E., Maloney, K. T., Barnett-Moore, N., Hosseinpour, M., and Bower, D. J.: Ocean basin evolution and global-scale plate reorganization events since Pangea breakup, Annual Review of Earth and Planetary

Sciences, 44, 107–138, https://doi.org/10.1146/annurev-earth-060115-012211, 2016.

Niederbockstruck, B., Jones, H. L., Yasukawa, K., Raffi, I., Tanaka, E., Westerhold, T., Ikehara, M., and Röhl, U.: Apparent diachroneity of calcareous nannofossil datums during the early Eocene in the high-latitude South Pacific Ocean. Paleoceanogr. Paleoclimatol., 39, e2023PA004801, https://doi.org/10.1029/2023PA004801, 2024.

Nocchi, M., Parisi, G., Monaco, P., Monechi, S., Madile, M., Napoleone, G., Ripepe, M., Orlando, M., Silva, I. P., and Bice, D. M.: The Eocene–Oligocene boundary in the Umbrian pelagic sequences, Italy, in: Developments in Palaeontology and Stratigraphy, Vol. 9, Elsevier, 25–40, https://doi.org/10.1016/S0920-5446(08)70091-8, 1986.

Norris, R. D.: Parallel evolution in the keel structure of planktonic foraminifera, J. Foraminifer. Res., 21, 319–331, 1991.

Norris, R. D.: Symbiosis as an evolutionary innovation in the radiation of Paleocene planktic foraminifera, Paleobiology, 22, 461–480, 1996.

Oberhänsli, H. and Beniamovskii, V. N.: Dysoxic bottom water events in the pero-Tethys during the late Ypresian: A result of changes in the evaporation/precipitation balance in adjacent continental regions, in: Early Paleogene warm climates and biosphere dynamics, edited by: Andreasson, F. P., Schmitz, B., and Thompson, E. I., Geologiska Foreningens i Stokholm Forhandlingar, 122, 121–123, 2000.

Olsson, R. K. and Hemleben, C.: Taxonomy, biostratigraphy, and phylogeny of Eocene Globanomalina, Planoglobanomalina n. gen., and Pseudohastigerina, in: Atlas of Eocene Planktonic Foraminifera, Cushman Foundation Special Publication 41, edited by: Pearson, P. N., Olsson, R. K., Huber, B. T., Hemleben, C., and Berggren, W. A., Cushman Foundation, ISBN 9781970168365, 2006.

Olsson, R. K., Pearson, P. N., Huber, B. T., and Berggren, W. A.: Taxonomy, biostratigraphy, and phylogeny of Eocene Globigerina, Globoturborotalita, Subbotina, and Turborotalita, in: Atlas of Eocene Planktonic Foraminifera, Cushman Foundation Special Publication 41, edited by: Pearson, P. N., Olsson, R. K., Huber, B. T., Hemleben, C., and Berggren, W. A., Cushman Foundation, 111–168, ISBN 9781970168365, 2006.

Parker, W. C. and Arnold, A. J.: Quantitative methods of data analysis in foraminiferal ecology, in: Modern Foraminifera, edited by: Sen Gupta, B. K., Kluwer Academic Publishers, Dordrecht, 74 pp., https://doi.org/10.1007/0-306-48104-9_5, 2003.

Parra, M., Mora, A., Jaramillo, C., Strecker, M. R., and Veloza, G.: New stratigraphic data on the initiation of mountain building at the eastern front of the Colombian Eastern Cordillera, in: International Symposium on Andean Geodynamics, Extended Abstracts, 567–571, ISBN 2-7099-1575-8, 2005.

Passchier, S., Bohaty, S. M., Jiménez-Espejo, F., Pross, J., Röhl, U., van de Flierdt, T., Escutia, C. and Brinkhuis, H.: Early Eocene to middle Miocene cooling and aridification of East Antarctica. Geochemistry, Geophysics, Geosystems, 14, 1399–1410, https://doi.org/10.1002/ggge.20106, 2013.

Pasley, M. A., Shepherd, D. B., Pocknall, D. T., Boyd, K. P., Vander, A., and Figueiredo, J. J. P.: Sequence stratigraphy and basin evolution of the Foz do Amazonas Basin, Brazil, Search and Discovery article no. 10082, http://www.searchanddiscovery.net/ (last access: 1 December 2025), 2005.

Pearson, P. N. and Berggren, W. A.: Taxonomy, biostratigraphy, and phylogeny of *Morozovelloides* n. gen., in: Atlas of Eocene Planktonic Foraminifera, Cushman Foundation Special Publication 41, edited by: Pearson, P. N., Olsson, R. K., Huber, B. T., Hemleben, C., and Berggren, W. A., Cushman Foundation, 327–342, ISBN 9781970168365, 2006.

Pearson, P. N. and Burgess, C. E.: Foraminifer test preservation and diagenesis: comparison of high latitude Eocene sites, in: Biogeochemical Controls on Palaeoceanographic Environmental Proxies, edited by: Austin, W. E. and James, R. H., Geol. Soc. Lond. Spec. Publ., 303, 59–72, 2008.

Pearson, P. N. and Wade, B. S.: Systematic taxonomy of exceptionally well-preserved planktonic foraminifera from the Eocene/Oligocene boundary of Tanzania, Special Publication 45, Cushman Foundation for Foraminiferal Research, 1–85, ISBN 9781970168402, 2015.

Pearson, P. N., Chaisson, W. P., Curry, W. B., Shackleton, N. J., and Richter, C.: Late Paleocene to middle Miocene planktonic foraminifer biostratigraphy of the Ceara Rise, in: Proceedings of the Ocean Drilling Program, Scientific Results, Vol. 154, Ocean Drilling Program College Station, Texas, USA, 33–68, https://doi.org/10.2973/odp.proc.sr.154.106.1997, 1997.

Pearson, P. N., Ditchfield, P. W., Singano, J., Harcourt-Brown, K. G., Nicholas, C. J., Olsson, R. K., Shackleton, N. J., and Hall, M. A.: Warm tropical sea surface temperatures in the Late Cretaceous and Eocene epochs, Nature, 413, 481–487, 2001.

Pearson, P. N., Evans, S. L., and Evans, J.: Effect of diagenetic recrystallization on the strength of planktonic foraminifer tests under compression, Geological Society of London, https://doi.org/10.1144/jmpaleo2013-032, 2015.

Pearson, P. N., Foster, G. L., and Wade, B. S.: Atmospheric carbon dioxide through the Eocene–Oligocene climate transition, Nature, 461, 1110–1113, https://doi.org/10.1038/nature08447, 2009.

Pearson, P. N., Nicholas, C. J., Singano, J. M., Bown, P. R., Coxall, H. K., van Dongen, B. E., Huber, B. T., Karega, A., Lees, J. A., Msaky, E., and Pancost, R. D. Paleogene and Cretaceous sediment cores from the Kilwa and Lindi areas of coastal Tanzania: Tanzania Drilling Project Sites 1–5, J. Afr. Earth Sci., 39, 25–62, 2004.

Pearson, P. N., Olsson, R. K., Huber, B. T., Hemleben, C., Berggren, W. A., and Coxall, H. K.: Overview of Eocene planktonic foraminiferal taxonomy, paleoecology, phylogeny, and biostratigraphy, in: Atlas of Eocene Planktonic Foraminifera, Cushman Foundation Special Publication 41, edited by: Pearson, P. N., Olsson, R. K., Huber, B. T., Hemleben, C., and Berggren, W. A., Cushman Foundation, 18–24, ISBN 9781970168365, 2006a.

Pearson, P. N., Olsson, R. K., Huber, B. T., Hemleben, C., and Berggren, W. A.: Atlas of Eocene Planktonic Foraminifera, in: Cushman Foundation Special Publication 41, Cushman Foundation, 1–513, ISBN 9781970168365, 2006b.

Pearson, P. N., Premec-Fucek, V., and Premoli Silva, I.: Taxonomy, biostratigraphy, and phylogeny of Eocene Turborotalia, in: Atlas of Eocene Planktonic Foraminifera, Cushman Foundation Special Publication 41, edited by: Pearson, P. N., Olsson, R. K., Huber, B. T., Hemleben, C., and Berggren, W. A., Cushman Foundation, 422–460, ISBN 9781970168365, 2006c.

Pearson, P. N., Olsson, R. K., Spezzaferri, S., and Leckie, R. M.: Taxonomy, biostratigraphy, and phylogeny of Oligocene

Globanomalinidae (Pseudohastigerina and Turborotalia), in: Atlas of Oligocene Planktonic Foraminifera, Cushman Foundation of Foraminiferal Research, Special Publication 46, edited by: Wade, B. S., Olsson, R. K., Pearson, P. N., Huber, B. T., and Berggren, W. A., Cushman Foundation, ISBN 9781970168365, 2018.

Pearson, P. N., Shackleton, N. J., and Hall, M. A.: Stable isotope paleoecology of middle Eocene planktonic foraminifera and multi-species isotope stratigraphy, DSDP Site 523, South Atlantic, The Journal of Foraminiferal Research, 23, 123–140, https://doi.org/10.2113/gsjfr.23.2.123, 1993.

Pearson, P. N., John, E., Wade, B. S., D'haenens, S., and Lear, C. H.: Spine-like structures in Paleogene muricate planktonic foraminifera, J. Micropalaeontol., 41, 107–127, https://doi.org/10.5194/jm-41-107-2022, 2022.

Pearson, P. N. and Wade, B. S.: Taxonomy and stable isotope paleoecology of well-preserved planktonic foraminifera from the uppermost Oligocene of Trinidad, The Journal of Foraminiferal Research, 39, 191–217, https://doi.org/10.2113/gsjfr.39.3.191, 2009.

Poore, R. Z. and Matthews, R. K.: Oxygen isotope ranking of Late Eocene and Oligocene planktonic foraminifers: implications for Oligocene sea-surface temperature and global ice volume, Mar. Micropalaeontol., 9, 111–134, 1984.

Premoli Silva, I., Orlando, M., Monechi, S., Madile, M., Napoleone, G., and Ripepe, M.: Calcareous plancton biostratigraphy and magnetostratigraphy at the Eocene–Oligocene transition in the Gubbio area, in: The Eocene–Oligocene Boundary in the Marche-Umbria Basin (Italy), International Subcommission on Paleogene Stratigraphy, stampa Aniballi, Ancona, 137–161, 1988.

Premoli Silva, I., Wade, B. S., and Pearson, P. N.: Taxonomy, biostratigraphy, and phylogeny of Globigerinatheka and Orbulinoides, in: Atlas of Eocene Planktonic Foraminifera, Cushman Foundation Special Publication 41, edited by: Pearson, P. N., Olsson, R. K., Huber, B. T., Hemleben, C., and Berggren, W. A., Cushman Foundation, 169–212, ISBN 9781970168365, 2006.

Pross, J., Contreras, L., Bijl, P. K., Greenwood, D. R., Bohaty, S. M., Schouten, S., Bendle, J. A., Röhl, U., Tauxe, L., Raine, J. I., and Huck, C. E.: Persistent near-tropical warmth on the Antarctic continent during the early Eocene epoch, Nature, 488, 73–77, https://doi.org/10.1038/nature11300, 2012.

Rae, J. W., Zhang, Y. G., Liu, X., Foster, G. L., Stoll, H. M., and Whiteford, R. D.: 2021. Atmospheric $CO_2$ over the past 66 million years from marine archives, Annual Review of Earth and Planetary Sciences, 49, 609–641, https://doi.org/10.1146/annurev-earth-082420-063026, 2021.

Renaudie, J., Danelian, T., Saint Martin, S., Le Callonnec, L., and Tribovillard, N.: Siliceous phytoplankton response to a Middle Eocene warming event recorded in the tropical Atlantic (Demerara Rise, ODP Site 1260A), Palaeogeogr. Palaeocl. Palaeoecol., 286, 121–134, 2010.

Rodrigues de Faria, G., Lazarus, D., Renaudie, J., Stammeier, J., Özen, V., and Struck, U.: Late Eocene to early Oligocene productivity events in the proto-Southern Ocean and correlation to climate change, Clim. Past, 20, 1327–1348, https://doi.org/10.5194/cp-20-1327-2024, 2024.

Saito, T.: Planktonic foraminifera biostratigraphy of eastern equatorial Pacific sediments, Deep-Sea Drilling Project Leg-85, Initial Reports of the Deep Sea Drilling Project, Texas A&M University, Ocean Drilling Program, College Station, TX, USA, 85, 621–653, https://doi.org/10.2973/dsdp.proc.85.116.1985, 1985.

Schiebel, R. and Hemleben, C.: Planktic foraminifers in the modern ocean (Vol. 358), Berlin: Springer, https://doi.org/10.1007/978-3-662-50297-6, 2017.

Schmidt, D. N., Thierstein, H. R., Bollmann, J., and Schiebel, R.: Abiotic forcing of plankton evolution in the Cenozoic, Science, 303, 207–210, https://doi.org/10.1126/science.1090592, 2004a.

Schmidt, D. N., Thierstein, H. R., and Bollmann, J.: The evolutionary history of size variation of planktic foraminiferal assemblages in the Cenozoic, Palaeogeogr. Palaeocl., 212, 159–180, 2004b.

Sexton, P. F., Wilson, P. A., and Pearson, P. N.: Microstructural and geochemical perspectives on planktic foraminiferal preservation: "Glassy" versus "Frosty", Geochem. Geophy. Geosy., 7, Q12P19, https://doi.org/10.1029/2006GC001291, 2006a.

Sexton, P. F., Wilson, P. A., and Pearson, P. N.: Palaeoecology of late middle Eocene planktic foraminifera and evolutionary implications, Mar. Micropaleontol., 60, 1–16, 2006b.

Shannon, C. E. and Weaver, W.: The Mathematical Theory of Communication, University of Illinois Press, Champaign, II, https://doi.org/10.1002/j.1538-7305.1948.tb01338.x, 1949.

Sloan, L. C. and Huber, M.: North Atlantic climate variability in the early Palaeogene: a climate modelling sensitivity study, in: Western North Atlantic Palaeogene and Cretaceous Palaeoceanography, edited by: Kroon, D., Norris, R. D., and Klaus, A., Geol. Soc. Spec. Publ., 183, 253–272, 2001a.

Sloan, L. C. and Huber, M.: Eocene oceanic response to orbital forcing on precessional time scales, Paleoceanography, 16, 101–111, 2001b.

Smart, C. W. and Thomas, E.: The enigma of early Miocene biserial planktic foraminifera, Geology, 34, 1041–1044, 2006.

Spezzaferri, S.: Planktonic foraminiferal biostratigraphy and taxonomy of the Oligocene and lower Miocene in the oceanic record. An Overview, Palaeontogr. Ital., 81, 1–187, 1994.

Spezzaferri, S., Olsson, R. K., Hemleben, C., Wade, B. S., and Coxall, H. K.: Taxonomy, biostratigraphy, and phylogeny of Oligocene and lower Miocene Globoturborotalita, in: Atlas of Oligocene Planktonic Foraminifera, Cushman Foundation of Foraminiferal Research, Special Publi55 cation 46, edited by: Wade, B. S., Olsson, R. K., Pearson, P. N., Huber, B. T., and Berggren, W. A., Cushman Foundation, ISBN 9781970168419, 2018.

Stott, L. D. and Kennett, J. P.: 34. Antarctic Paleogene planktonic foraminifer biostratigraphy: ODP Leg 113, Sites 689 and 690, edited by: Barker, P. F. and Kennett, J. P., Proc. Ocean Drill. Prog., 113, 549–569, 1990.

Swain, A., Woodhouse, A., Fagan, W. F., Fraass, A. J., and Lowery, C. M.: Biogeographic response of marine plankton to Cenozoic environmental changes, Nature, 629, 616–623, 2024.

Thomas, E.: Descent into the Icehouse, Geology, 36, 191–192, 2008.

Toumoulin, A., Tardif, D., Donnadieu, Y., Licht, A., Ladant, J.-B., Kunzmann, L., and Dupont-Nivet, G.: Evolution of continental temperature seasonality from the Eocene greenhouse to the Oligocene icehouse – a model–data comparison, Clim. Past, 18, 341–362, https://doi.org/10.5194/cp-18-341-2022, 2022.

van Andel, T. H., and Moore Jr., T. C.: Cenozoic calcium carbonate distribution and calcite compensation depth in the central equatorial Pacific Ocean, Geology, 2, 87–92, 1974.

Vandenberghe, N., Hilgen, F. J., and Speijer, R. P.: The Paleogene Period, Chapter 28, in: The Geologic Time Scale 2012, Vol. 2, edited by: Gradstein, F. M., Ogg, J. G., Schmitiz, M. D., and Ogg, G. M., Elsevier, Amsterdam, 855–922, https://doi.org/10.1016/B978-0-444-59425-9.00028-7, 2012.

van der Zwaan, G. J., Jorissen, F. J., and de Stigter, H. C.: The depth dependency of planktonic/benthic foraminiferal ratios: Constraints and applications, Mar. Geol., 95, 1–16, 1990.

Van Eijden, A. J. M. and Ganssen, G. M.: An Oligocene multispecies foraminiferal oxygen and carbon isotope record from ODP Hole 758A (Indian Ocean): paleoceanographic and paleoecologic implications, Marine Micropaleontology, 25, 47–65, https://doi.org/10.1016/0377-8398(94)00028-L, 1995.

Varol O.: Nannofossil Biostratigraphy of BP Offshore Well, Internal Report, Agência Nacional do Petróleo, Gás Natural e Biocombustíveis, Brazil, 2004.

Wade, B. S.: Planktonic foraminiferal biostratigraphy and mechanisms in the extinction of Morozovella in the late Middle Eocene, Mar. Micropaleontol., 51, 23–38, 2004.

Wade, B. S., Al-Sabouni, N., Hemleben, C., and Kroon, D.: Symbiont bleaching in fossil planktonic foraminifera, Evolutionary Ecology, 22, 253–265, https://doi.org/10.1007/s10682-007-9176-6, 2008.

Wade, B. S. and Cheng, N. K.: No paleoclimatic anomalies are associated with the late Eocene extraterrestrial impact events, Commun. Earth Environ., 5, 710, https://doi.org/10.1038/s43247-024-01874-x, 2024.

Wade, B. S. and Olsson, R. K.: Investigation of pre-extinction dwarfing in Cenozoic planktonic foraminifera, Palaeogeogr. Palaeocl. Palaeoecol., 284, 39–46, 2009.

Wade, B. S. and Pearson, P. N.: Planktonic foraminiferal turnover, diversity fluctuations and geochemical signals across the Eocene/Oligocene boundary in Tanzania, Mar. Micropaleontol., 68, 244–255, 2008.

Wade, B. S., Pearson, P. N., Berggren, W. A., and Pälike, H.: Review and revision of Cenozoic tropical planktonic foraminiferal biostratigraphy and calibration to the geomagnetic polarity and astronomical time scale, Earth-Sci. Rev., 104, 111–142, 2011.

Wade, B. S., Houben, A. J. P., Quaijtaal, W., Schouten, S., Rosenthal, Y., Miller, K. G., Katz, M. E., Wright, J. D., and Brinkhuis, H.: Multiproxy record of abrupt sea-surface cooling across the Eocene–Oligocene transition in the Gulf of Mexico, Geology, 40, 159–162, 2012.

Wade, B. S., Pearson, P. N., Olsson, R. K., Premoli Silva, I., Berggren, W. A., Spezzaferri, S., Huber, B. T., Coxall, H. K., Premec-Fucek, V., Hernitz Kucenjak, M., Hemleben, C., Leckie, R. M., and Smart, C. W.: Taxonomy, biostratigraphy, phylogeny, and diversity of Oligocene and early Miocene planktonic foraminifera, in: Atlas of Oligocene Planktonic Foraminifera, Cushman Foundation of Foraminiferal Research, Special Publication 46, edtied by: Wade, B. S., Olsson, R. K., Pearson, P. N., Huber, B. T., and Berggren, W. A., Cushman Foundation, 11–28, ISBN 9781970168419, 2018a.

Wade, B. S., Olsson, R. K., Pearson, P. N., Huber, B. T., and Berggren, W. A. (Eds.): Atlas of Oligocene Planktonic Foraminifera, in: Cushman Foundation Special Publication 46, Cushman Foundation, 528 pp., ISBN 9781970168419, 2018b.

Wade, B. S., Olsson, R. K. Pearson, P. N., Edgar, K. M., and Premoli Silva, I.: Taxonomy, biostratigraphy, and phylogeny of Oligocene *Subbotina*, in: Atlas of Oligocene Planktonic Foraminifera, Cushman Foundation of Foraminiferal Research, Special Publication 46, edited by: Wade, B. S., Olsson, R. K., Pearson, P. N., Huber, B. T., and Berggren, W. A., Cushman Foundation, 307–330, ISBN 9781970168419, 2018c.

Wade, B. S., Pearson, P. N., Olsson, R. K., Fraass, A. Leckie, R. M., and Hemleben, C.: Taxonomy, biostratigraphy, and phylogeny of Oligocene and lower Miocene *Dentoglobigerina* and *Globoquadrina*, in: Atlas of Oligocene Planktonic Foraminifera, Cushman Foundation of Foraminiferal Research, Special Publication 46, edited by: Wade, B. S., Olsson, R. K., Pearson, P. N., Huber, B. T., and Berggren, W. A., Cushman Foundation, 331–384, ISBN 9781970168419, 2018d.

Wade, B. S., Aljahdali, M. H., Mufrreh, Y. A., Memesh, A. M., AlSoubhi, S. A., and Zalmout, I. S.: Upper Eocene planktonic foraminifera from northern Saudi Arabia: implications for stratigraphic ranges, J. Micropalaeontol., 40, 145–161, 2021.

Walker, M.: Linking shape and sinking speed in planktonic Foraminifera, Doctoral dissertation, University of Lincoln, https://doi.org/10.24385/lincoln.24326140, 2019.

Waterson, A. M., Edgar, K. M., Schmidt, D. N., and Valdes, P. J.: Quantifying the stability of planktic foraminiferal physical niches between the Holocene and Last Glacial Maximum, Paleoceanography, 32, 74–89, 2017.

Westerhold, T., Marwan, N., Drury, A. J., Liebrand, D., Agnini, C., Anagnostou, E., Barnet, J. S., Bohaty, S. M., De Vleeschouwer, D., Florindo, F., and Frederichs, T.: An astronomically dated record of Earth's climate and its predictability over the last 66 million years. science, 369, 1383–1387, https://doi.org/10.1126/science.aba6853, 2020.

Winterer, E. L., Riedel, W. R., Moberly, R. M., Resig Jr., J. M., Kroenke, L. W., Gealy, E. L., Heath, G. R., Brönnimann, P., Martini, E., and Worsley, T. R.: Site 64, in: Initial reports of the Deep Sea Drilling Project covering Leg 7 of the cruises of the drilling vessel Glomar Challenger, Apra, Guam to Honolulu, Hawaii, August–September 1969, Initial Reports of the Deep Sea Drilling Project, Vol. 7, Part 1, edited by: Winterer, E. L., Riedel, W. R., Brönnimann, P., Gealy, E. L., Heath, G. R., Kroenke, L. W., Martini, E., Moberly Jr., R., Resig, J. M., and Worsley, T. R., Texas A&M University, Ocean Drilling Program, College Station, TX, USA, 473–606, https://doi.org/10.2973/dsdp.proc.7.106.1971, 1971.

Witkowski, J., Penman, D. E., Bryłka, K., Wade, B. S., Matting, S., Harwood, D. M., and Bohaty, S. M.: Early Paleogene biosiliceous sedimentation in the Atlantic Ocean: Testing the inorganic origin hypothesis for Paleocene and Eocene chert and porcellanite, Palaeogeogr. Palaeocl. Palaeoecol., 556, 109896, https://doi.org/10.1016/j.palaeo.2020.109896, 2020.

Witkowski, J., Bryłka, K., Bohaty, S. M., Mydłowska, E., Penman, D. E., and Wade, B. S.: North Atlantic marine biogenic silica accumulation through the early to middle Paleogene: implications for ocean circulation and silicate weathering feedback, Clim. Past, 17, 1937–1954, https://doi.org/10.5194/cp-17-1937-2021, 2021.

Woodhouse, A.: Evolutionary dynamics of Cenozoic planktonic foraminifera: insights from biogeography, geochemistry, and morphology, Doctoral dissertation, University of Leeds, 2021.

Woodhouse, A.: Palaeobiology: Emergence of the Southern Ocean, Curr. Biol., 35, R104–R107, 2025.

Woodhouse, A., Jackson, S. L., Jamieson, R. A., Newton, R. J., Sexton, P. F., and Aze, T.: Adaptive ecological niche migration does not negate extinction susceptibility, Sci. Rep., 11, 15411, https://doi.org/10.1038/s41598-021-94140-5, 2021.

Woodhouse, A., Procter, F. A., Jackson, S. L., Jamieson, R. A., Newton, R. J., Sexton, P. F., and Aze, T.: Paleoecology and evolutionary response of planktonic foraminifera to the mid-Pliocene Warm Period and Plio-Pleistocene bipolar ice sheet expansion, Biogeosciences, 20, 121–139, https://doi.org/10.5194/bg-20-121-2023, 2023a.

Woodhouse, A., Swain, A., Fagan, W. F., Fraass, A. J., and Lowery, C. M.: Late Cenozoic cooling restructured global marine plankton communities, Nature, 614, 713–718, https://doi.org/10.1038/s41586-023-05694-5, 2023b.

Yasuhara, M. and Deutsch, C. A.: Tropical biodiversity linked to polar climate, Nature, 614, 626–628, 2023.

Zachos, J. C., Pagani, M., Sloan, L., Thomas, E., and Billups, K.: Trends, rhythms, and aberrations in global climate 65 Ma to present, Science, 292, 686–693, 2001.

Zhang, Y. G., Pagani, M., Liu, Z., Bohaty, S. M., and DeConto, R.: A 40-million-year history of atmospheric CO2, Philosophical Transactions of the Royal Society A: Mathematical, Physical and Engineering Sciences, 371, 20130096, 2013.